Satellite dynamics on the Laplace surface

Scott Tremaine[1], Jihad Touma[2], and Fathi Namouni[3]

ABSTRACT

The orbital dynamics of most planetary satellites is governed by the quadrupole moment from the equatorial bulge of the host planet and the tidal field from the Sun. On the Laplace surface, the long-term orbital evolution driven by the combined effects of these forces is zero, so that orbits have a fixed orientation and shape. The "classical" Laplace surface is defined for circular orbits, and coincides with the planet's equator at small planetocentric distances and with its orbital plane at large distances. A dissipative circumplanetary disk should settle to this surface, and hence satellites formed from such a disk are likely to orbit in or near the classical Laplace surface. This paper studies the properties of Laplace surfaces. Our principal results are: (i) if the planetary obliquity exceeds 68.875° there is a range of semimajor axes in which the classical Laplace surface is unstable; (ii) at some obliquities and planetocentric distances there is a distinct Laplace surface consisting of nested eccentric orbits, which bifurcates from the classical Laplace surface at the point where instability sets in; (ii) there is also a "polar" Laplace surface perpendicular to the line of nodes of the planetary equator on the planetary orbit; (iv) for circular orbits, the polar Laplace surface is stable at small planetocentric distances and unstable at large distances; (v) at the onset of instability this polar Laplace surface bifurcates into two polar Laplace surfaces composed of nested eccentric orbits.

Subject headings: planets and satellites: formation – planets and satellites: general

[1]School of Natural Sciences, Institute for Advanced Study, Einstein Drive, Princeton, NJ 08540, USA; tremaine@ias.edu

[2]Department of Physics, American University of Beirut, PO Box 11–0236, Riad El-Solh, Beirut 1107 2020, Lebanon; jihad.touma@gmail.com

[3]Université de Nice and CNRS, Observatoire de la Côte d'Azur, BP 4229, 06304 Nice, France; namouni@obs-nice.fr

1. Introduction

In his study of Jupiter's satellites, Laplace (1805) recognized that the combined effects of the solar tide and the planet's oblateness induced a "proper" inclination in satellite orbits with respect to Jupiter's equator. He remarked that this proper inclination increases with the distance to the planet, and defines an orbital plane for circular orbits that lies between the orbital plane of the planet's motion round the Sun and its equator plane. This plane is called the Laplace plane.

More generally, the Laplace plane is usually defined as the plane normal to the axis about which the pole of a satellite's orbit precesses[1]. The "Laplace surface" is the locus of all orbits that do not precess (i.e., the secular motion of the node and apse vanishes).

In the most common situation, we consider circular satellite orbits around an oblate planet with non-zero obliquity, traveling around the Sun. The Laplace surface is then determined by the competition between the interior quadrupole potential from the equatorial bulge and the external quadrupole potential from the Sun. Close to the planet, the "classical" Laplace surface nearly coincides with the planetary equator, while at large distances it nearly coincides with the planetary orbital plane. The transition between these two orientations occurs near the "Laplace radius," defined below in equation (24).

The Laplace surface is important because it traces the shape expected for a thin gas disk or dissipative particulate ring surrounding the planet. Thus it is not surprising that many planetary satellites orbit close to the Laplace surface; those that do probably formed from a circumplanetary gas disk while those that do not were presumably either captured from heliocentric orbits or experienced unusual events in their past history.

The purpose of this paper is to study the properties of the Laplace surface, including the stability of is generating orbits and its generalization to eccentric orbits. Although the Laplace surface has been known and studied for over two centuries, we believe that many of the results we present are new.

[1]Unfortunately, the term is sometimes also applied to the invariable plane, the plane perpendicular to the total angular momentum of an N-body system.

2. Secular equations of motion

2.1. The Hamiltonian

The Kepler Hamiltonian that describes the motion of a test particle orbiting an isolated point mass M is

$$H_K = \tfrac{1}{2}v^2 - \frac{GM}{r} = -\frac{GM}{2a}; \tag{1}$$

here $\mathbf{r}$ is the position vector measured from the center of the planet, $\mathbf{v} = \dot{\mathbf{r}}$, $r = |\mathbf{r}|$, and a is the semimajor axis of the test particle. The constants of motion are the Hamiltonian H_K (or semimajor axis a), and the angular momentum and eccentricity vectors

$$\mathbf{L} = \mathbf{r} \times \mathbf{v}, \quad \mathbf{e} = \frac{1}{GM}\mathbf{v} \times (\mathbf{r} \times \mathbf{v}) - \frac{\mathbf{r}}{r}; \tag{2}$$

these are related to the eccentricity e and semimajor axis of the orbit by $L^2 = GMa(1 - e^2)$ and $|\mathbf{e}| = e$.

We now examine how the motion of the test particle is affected by additional forces from the equatorial bulge of the planet and the Sun. The quadrupole potential arising from an oblate planet is

$$\Phi_p(\mathbf{r}) = \frac{GMJ_2R_p^2}{r^3}P_2(\cos\theta) = \frac{GMJ_2R_p^2}{2r^5}[3(\mathbf{r}\cdot\mathbf{n}_p)^2 - r^2], \tag{3}$$

where J_2 is the quadrupole gravitational harmonic, R_p is the planetary radius, $P_2(x) = \frac{1}{2}(3x^2 - 1)$ is a Legendre polynomial, and θ is the polar angle measured from the planet's spin axis, which is oriented along the unit vector $\mathbf{n}_p$.

The quadrupole potential of the planet may be enhanced by inner satellites. If the planet hosts n satellites with masses m_i, $i = 1, \ldots, n$, on circular orbits in the equatorial plane of the planet with semimajor axes a_i, then at distances $r \gg a_i$ the gravitational potential due to the satellites can be accounted for by augmenting J_2 to J_2', where

$$J_2'R_p^2 \equiv J_2R_p^2 + \tfrac{1}{2}\sum_{i=1}^{n} a_i^2 m_i/M. \tag{4}$$

Values of J_2 and J_2' for the giant planets and Pluto are given in Table 1.

Since the solar tide is assumed to be weak, we may estimate its effects by averaging over the solar orbital period. We assume that the planetary orbit has semimajor axis $a_\odot$ and eccentricity $e_\odot$, and denote the normal to the orbit by the unit vector $\mathbf{n}_\odot$. The obliquity of

the planet is then $\phi_\odot = \cos^{-1} \mathbf{n}_\odot \cdot \mathbf{n}_p$. Since $r \ll a_\odot$ we need keep only the quadrupole term in the averaged solar potential,

$$\Phi_\odot(\mathbf{r}) = \frac{GM_\odot}{4a_\odot^3(1-e_\odot^2)^{3/2}}[3(\mathbf{r}\cdot\mathbf{n}_\odot)^2 - r^2]. \tag{5}$$

The solar tide also causes the spin axis of the planet to precess, through its torque on the equatorial bulge. We neglect this effect to keep the analysis simple, since the precession rate of the planetary spin due to solar tides is normally much smaller than the precession rate of the satellite orbit (see Goldreich 1965 and Boué & Laskar 2006 for treatments that include precession of the planetary spin).

The planet's "radius of influence" or "Hill radius" is

$$r_H = a_\odot \left(\frac{M}{3M_\odot}\right)^{1/3}. \tag{6}$$

The Hill radius is roughly the point at which $|\Phi_\odot| \sim GM/r$; beyond the Hill radius the gravitational force experienced by a satellite is dominated by the solar tide rather than the force from the planet and most orbits are not bound to the planet. The Hill radius also marks the location of the collinear Lagrange points of the planet (Murray & Dermott 1999). Our use of the orbit-averaged solar potential requires that the satellite radius $r \ll r_\mathrm{H}$.

The total non-Keplerian potential due to the oblate planet, inner satellites, and Sun is $\Phi = \Phi_p + \Phi_\odot$.

Now average over the Keplerian orbit of the test particle, which has semimajor axis a, eccentricity e, and orientation specified by the unit vectors $\mathbf{n}$ along the angular momentum vector, $\mathbf{u}$ towards pericenter, and $\mathbf{v} = \mathbf{n}\times\mathbf{u}$. We have

$$\langle r^2\rangle = a^2(1+\tfrac{3}{2}e^2), \quad \langle(\mathbf{r}\cdot\mathbf{u})^2\rangle = a^2(\tfrac{1}{2}+2e^2), \quad \langle(\mathbf{r}\cdot\mathbf{v})^2\rangle = a^2(\tfrac{1}{2}-\tfrac{1}{2}e^2), \tag{7}$$

$$\left\langle\frac{1}{r^3}\right\rangle = \frac{1}{a^3(1-e^2)^{3/2}}, \quad \left\langle\frac{(\mathbf{r}\cdot\mathbf{u})^2}{r^5}\right\rangle = \left\langle\frac{(\mathbf{r}\cdot\mathbf{v})^2}{r^5}\right\rangle = \frac{1}{2a^3(1-e^2)^{3/2}}. \tag{8}$$

The averaged potential is $\overline{\Phi} \equiv \overline{\Phi}_p + \overline{\Phi}_\odot$, where

$$\begin{aligned} \overline{\Phi}_p \equiv \langle\Phi_p\rangle &= \frac{GMJ_2'R_p^2}{4a^3(1-e^2)^{3/2}}\left[1-3(\mathbf{n}_p\cdot\mathbf{n})^2\right], \\ \overline{\Phi}_\odot \equiv \langle\Phi_\odot\rangle &= \frac{3GM_\odot a^2}{4a_\odot^3(1-e_\odot^2)^{3/2}}\left[(\tfrac{1}{2}+2e^2)(\mathbf{n}_\odot\cdot\mathbf{u})^2 + (\tfrac{1}{2}-\tfrac{1}{2}e^2)(\mathbf{n}_\odot\cdot\mathbf{v})^2 - \tfrac{1}{2}e^2 - \tfrac{1}{3}\right]. \end{aligned} \tag{9}$$

The averaged Hamiltonian is then

$$H = H_K + \overline{\Phi}_p + \overline{\Phi}_\odot. \tag{10}$$

By virtue of the orbit averaging, this Hamiltonian is independent of the mean anomaly, so its conjugate momentum $(GMa)^{1/2}$ is a constant of motion, which in turn means that the semimajor axis may be treated as a constant.

Now set

$$\mathbf{j} \equiv (1-e^2)^{1/2}\mathbf{n}, \qquad \mathbf{e} = e\mathbf{u}, \qquad \tau = \sqrt{\frac{GM}{a^3}}t, \qquad \epsilon_\odot = \frac{M_\odot a^3}{Ma_\odot^3(1-e_\odot^2)^{3/2}}, \qquad \epsilon_p = \frac{J_2' R_p^2}{a^2}. \tag{11}$$

The angular momentum $\mathbf{L} = (GMa)^{1/2}\mathbf{j}$ and, as suggested by the notation, $\mathbf{e}$ is the eccentricity vector (eq. 2). If we define a dimensionless potential $\Psi_p + \Psi_\odot = (\overline{\Phi}_p + \overline{\Phi}_\odot)a/(GM)$, we have

$$\begin{aligned} \Psi_p &= \frac{\epsilon_p}{4(1-e^2)^{5/2}}\left[1 - e^2 - 3(\mathbf{j}\cdot\mathbf{n}_p)^2\right], \\ \Psi_\odot &= \frac{3\epsilon_\odot}{8}\left[5(\mathbf{e}\cdot\mathbf{n}_\odot)^2 - (\mathbf{j}\cdot\mathbf{n}_\odot)^2 - 2e^2\right]; \end{aligned} \tag{12}$$

an unimportant constant has been dropped.

To repeat, the Hamiltonian $H_K + GM(\Psi_p + \Psi_\odot)/a$ is based on the assumptions that (i) the precession rate of the planetary spin due to solar tides is negligible; (ii) the satellite is a massless test particle; (iii) the Sun is far enough from the planet that the solar tide can be approximated by a quadrupole; (iv) the satellite is far enough from the planet that the potential from the planet and the inner satellites can be approximated as a a monopole plus a quadrupole; (v) the perturbing forces due to $\Psi_p + \Psi_\odot$ are weak enough that the secular equations of motion can be used to describe its orbital evolution.

2.2. Equations of motion

Using equation (2) it is straightforward to show that the Poisson brackets of $\mathbf{j}$ and $\mathbf{e}$ are

$$\{j_i, j_j\} = \frac{1}{\sqrt{GMa}}\epsilon_{ijk}j_k, \quad \{e_i, e_j\} = \frac{1}{\sqrt{GMa}}\epsilon_{ijk}j_k, \quad \{j_i, e_j\} = \frac{1}{\sqrt{GMa}}\epsilon_{ijk}e_k, \tag{13}$$

where ϵ_{ijk} is the antisymmetric tensor.

The time evolution of any variable f determined by the Hamiltonian H is given by

$$\frac{df}{dt} = \{f, H\}. \tag{14}$$

In secular dynamics the semimajor axis is fixed and H can be considered to be a function only of the shape of the orbit, as expressed by $\mathbf{j}$ and $\mathbf{e}$. Then from the chain rule

$$\frac{df}{dt} = \{f, \mathbf{j}\}\boldsymbol{\nabla}_{\mathbf{j}}H + \{f, \mathbf{e}\}\boldsymbol{\nabla}_{\mathbf{e}}H, \tag{15}$$

where $\nabla_{\mathbf{j}}$ is the vector $(\partial/\partial j_1, \partial/\partial j_2, \partial/\partial j_3)$ with a similar definition for $\nabla_{\mathbf{e}}$. Replacing f successively by j_i and e_i and using the relations (13), we find

$$\begin{aligned}\frac{d\mathbf{j}}{dt} &= -\frac{1}{\sqrt{GMa}}\left(\mathbf{e}\times\nabla_{\mathbf{e}}H + \mathbf{j}\times\nabla_{\mathbf{j}}H\right)\\ \frac{d\mathbf{e}}{dt} &= -\frac{1}{\sqrt{GMa}}\left(\mathbf{j}\times\nabla_{\mathbf{e}}H + \mathbf{e}\times\nabla_{\mathbf{j}}H\right).\end{aligned} \tag{16}$$

Since $\mathbf{e}$ and $\mathbf{j}$ are constants of motion for the Kepler Hamiltonian H_K, the contribution of H_K to the right side of this equation must vanish, so we can replace $H = H_K + \overline{\Phi}$ by $\overline{\Phi}$. Equations (16) date back to Milankovich (1939, eqs. 204 and 205; see also Breiter & Ratajczak 2005 and references therein).

These equations admit three integrals of motion, $\overline{\Phi}$, $\mathbf{j}\cdot\mathbf{e}$ and $\mathbf{j}^2+\mathbf{e}^2$. Physically meaningful solutions are restricted to the four-dimensional manifold on which

$$\mathbf{j}\cdot\mathbf{e} = 0, \qquad \mathbf{j}^2 + \mathbf{e}^2 = 1. \tag{17}$$

Replacing t and Φ by the dimensionless variables τ and Ψ defined in equation (11) we obtain[2]

$$\begin{aligned}\frac{d\mathbf{j}}{d\tau} &= -\mathbf{j}\times\nabla_{\mathbf{j}}\Psi - \mathbf{e}\times\nabla_{\mathbf{e}}\Psi,\\ \frac{d\mathbf{e}}{d\tau} &= -\mathbf{e}\times\nabla_{\mathbf{j}}\Psi - \mathbf{j}\times\nabla_{\mathbf{e}}\Psi.\end{aligned} \tag{18}$$

For the potential given by equations (12) we finally have

$$\begin{aligned}\frac{d\mathbf{j}}{d\tau} &= \frac{3\epsilon_\odot\,\mathbf{j}\cdot\mathbf{n}_\odot}{4}\mathbf{j}\times\mathbf{n}_\odot - \frac{15\epsilon_\odot\,\mathbf{e}\cdot\mathbf{n}_\odot}{4}\mathbf{e}\times\mathbf{n}_\odot + \frac{3\epsilon_p\,\mathbf{j}\cdot\mathbf{n}_p}{2(1-e^2)^{5/2}}\mathbf{j}\times\mathbf{n}_p,\\ \frac{d\mathbf{e}}{d\tau} &= \frac{3\epsilon_\odot\,\mathbf{j}\cdot\mathbf{n}_\odot}{4}\mathbf{e}\times\mathbf{n}_\odot - \frac{15\epsilon_\odot\,\mathbf{e}\cdot\mathbf{n}_\odot}{4}\mathbf{j}\times\mathbf{n}_\odot + \frac{3\epsilon_p\,\mathbf{j}\cdot\mathbf{n}_p}{2(1-e^2)^{5/2}}\mathbf{e}\times\mathbf{n}_p\\ &\quad + \left[\tfrac{3}{2}\epsilon_\odot - \tfrac{3}{4}\epsilon_p\frac{1-e^2-5(\mathbf{j}\cdot\mathbf{n}_p)^2}{(1-e^2)^{7/2}}\right]\mathbf{j}\times\mathbf{e}.\end{aligned} \tag{19}$$

To avoid distraction by trivial cases, we shall always assume that $\epsilon_p > 0$ (the planetary quadrupole is non-zero and positive, as expected for a planet that is oblate or has inner satellites), $\epsilon_\odot > 0$ (solar perturbations are non-negligible), and $\mathbf{n}_\odot$ is neither parallel, antiparallel,

[2] There is a gauge freedom in the definition of $\Psi(\mathbf{j},\mathbf{e})$ since the variables $\mathbf{j}$ and $\mathbf{e}$ are related by (17). It is shown in Appendix A that the secular equations of motion (18) are independent of gauge.

or perpendicular to $\mathbf{n}_p$ (the planetary obliquity is not $0, \pm\frac{1}{2}\pi, \pi$). The plane defined by the planetary spin axis $\mathbf{n}_p$ and the normal to the solar orbit $\mathbf{n}_\odot$ will be called the principal plane.

We shall sometimes use cylindrical coordinates with the z-axis oriented along $\mathbf{n}_p \times \mathbf{n}_\odot$, so the plane $z = 0$ coincides with the principal plane. The positive x-axis is chosen to coincide with $\mathbf{n}_p$. Then $\mathbf{n}_\odot$ lies in the $z = 0$ plane, so it may be specified by its azimuthal angle $\phi_\odot$ (the obliquity), which lies in the range $(0, \pi)$.

In the limit $\epsilon_p \to 0$ equations (19) provide a vector description of Kozai oscillations, the secular oscillations in the eccentricity and inclination of (for example) a planet orbiting a member of a binary star (Kozai 1962; Holman et al. 1997; Ford et al. 2000).

Equations (19) are invariant under the transformations

$$\mathbf{e} \to -\mathbf{e} \quad \text{or} \quad \mathbf{n}_\odot \to -\mathbf{n}_\odot \quad \text{or} \quad \mathbf{n}_p \to -\mathbf{n}_p \quad \text{or} \quad (\mathbf{j} \to -\mathbf{j}, \tau \to -\tau). \tag{20}$$

Invariance under $\mathbf{n}_\odot \to -\mathbf{n}_\odot$ implies that we can restrict the range of the obliquity $\phi_\odot$ from $(0, \pi)$ to $(0, \frac{1}{2}\pi)$.

Recall that equations (19) hold for arbitrary eccentricity, i.e., they do not represent an expansion that is valid only for $e \ll 1$.

We define the Laplace equilibria to be stationary solutions of equations (19), and the Laplace surface(s) to be the locus of all orbits that are Laplace equilibria.

3. Circular Laplace equilibria

The equations of motion (19) can be solved explicitly in the case of circular orbits ($\mathbf{e} = 0$). We banish this discussion to Appendix B and focus in this section on the equilibrium solutions, with $\mathbf{e} = 0$ and $\mathbf{j}$ =constant, which we call the circular Laplace equilibria.

In circular Laplace equilibria the second of equations (19) is satisfied trivially. The first of equations (19) yields

$$\epsilon_\odot(\mathbf{j} \cdot \mathbf{n}_\odot)\mathbf{j} \times \mathbf{n}_\odot + 2\epsilon_p(\mathbf{j} \cdot \mathbf{n}_p)\mathbf{j} \times \mathbf{n}_p = 0. \tag{21}$$

Taking the scalar product of this equation with $\mathbf{n}_\odot$, and again with $\mathbf{n}_p$, we conclude that either (i) $\mathbf{j} \cdot \mathbf{n}_p = \mathbf{j} \cdot \mathbf{n}_\odot = 0$; (ii) $\mathbf{j} \cdot (\mathbf{n}_p \times \mathbf{n}_\odot) = 0$. In the first case $\mathbf{j}$ is perpendicular to the principal plane, and we call this the "orthogonal" or "circular orthogonal" Laplace equilibrium; in the second case $\mathbf{j}$ lies in the principal plane and we call this the "coplanar" or "circular coplanar" Laplace equilibrium.

In the coplanar Laplace equilibrium, $\mathbf{j}$ lies in the $z = 0$ plane, so it may be specified by its azimuthal angle ϕ. The equilibrium condition (21) becomes

$$\epsilon_\odot \sin 2(\phi - \phi_\odot) + 2\epsilon_p \sin 2\phi = 0. \tag{22}$$

This equation has four solutions for ϕ in a 2π interval; if ϕ is a solution then $\phi \pm \frac{1}{2}\pi$ and $\phi + \pi$ are also solutions.

Equation (22) may also be written as

$$a^5 \sin 2(\phi - \phi_\odot) + 2r_L^5 \sin 2\phi = 0, \tag{23}$$

where the Laplace radius r_L is defined by

$$r_L^5 = J_2' R_p^2 a_\odot^3 (1 - e_\odot^2)^{3/2} \frac{M}{M_\odot}. \tag{24}$$

3.1. Stability

The stability of the circular Laplace equilibria can be determined by writing $\mathbf{j} = \mathbf{j}_0 + \mathbf{j}_1$ and expanding equations (19) to first order in $\mathbf{j}_1$ and $\mathbf{e}$:

$$\begin{aligned}
\frac{d\mathbf{j}_1}{d\tau} &= \frac{3\epsilon_\odot \mathbf{j}_1 \cdot \mathbf{n}_\odot}{4}\mathbf{j}_0 \times \mathbf{n}_\odot + \frac{3\epsilon_\odot \mathbf{j}_0 \cdot \mathbf{n}_\odot}{4}\mathbf{j}_1 \times \mathbf{n}_\odot + \frac{3\epsilon_p \mathbf{j}_1 \cdot \mathbf{n}_p}{2}\mathbf{j}_0 \times \mathbf{n}_p + \frac{3\epsilon_p \mathbf{j}_0 \cdot \mathbf{n}_p}{2}\mathbf{j}_1 \times \mathbf{n}_p, \\
\frac{d\mathbf{e}}{d\tau} &= \frac{3\epsilon_\odot \mathbf{j}_0 \cdot \mathbf{n}_\odot}{4}\mathbf{e} \times \mathbf{n}_\odot - \frac{15\epsilon_\odot \mathbf{e} \cdot \mathbf{n}_\odot}{4}\mathbf{j}_0 \times \mathbf{n}_\odot + \frac{3\epsilon_p \mathbf{j}_0 \cdot \mathbf{n}_p}{2}\mathbf{e} \times \mathbf{n}_p \\
&\qquad + \left\{\tfrac{3}{2}\epsilon_\odot - \tfrac{3}{4}\epsilon_p[1 - 5(\mathbf{j}_0 \cdot \mathbf{n}_p)^2]\right\} \mathbf{j}_0 \times \mathbf{e}.
\end{aligned} \tag{25}$$

Note that the two equations are decoupled: the linearized evolution of the orientation of the orbital plane, specified by $\mathbf{j}$, is independent of the linearized evolution of the eccentricity and apse direction, specified by $\mathbf{e}$.

It is easy to show using the equilibrium equation (21) that a trivial solution of the first of these equations is $\mathbf{j}_1 = k\mathbf{j}_0$ where $k \ll 1$ is a constant. In other words, the eigenvalue equation in λ obtained by assuming $\mathbf{j}_1 \propto \exp(\lambda t)$ always has one zero eigenvalue. This is an unphysical solution of the linearized equations since the constant of motion $\mathbf{j}^2 + \mathbf{e}^2 = 1$ requires that $\mathbf{j}_0 \cdot \mathbf{j}_1 = 0$.

3.1.1. The circular orthogonal Laplace equilibrium

In the orthogonal equilibrium equations (25) simplify to

$$\frac{d\mathbf{j}_1}{d\tau} = \frac{3\epsilon_\odot \mathbf{j}_1 \cdot \mathbf{n}_\odot}{4}\mathbf{j}_0 \times \mathbf{n}_\odot + \frac{3\epsilon_p \mathbf{j}_1 \cdot \mathbf{n}_p}{2}\mathbf{j}_0 \times \mathbf{n}_p,$$

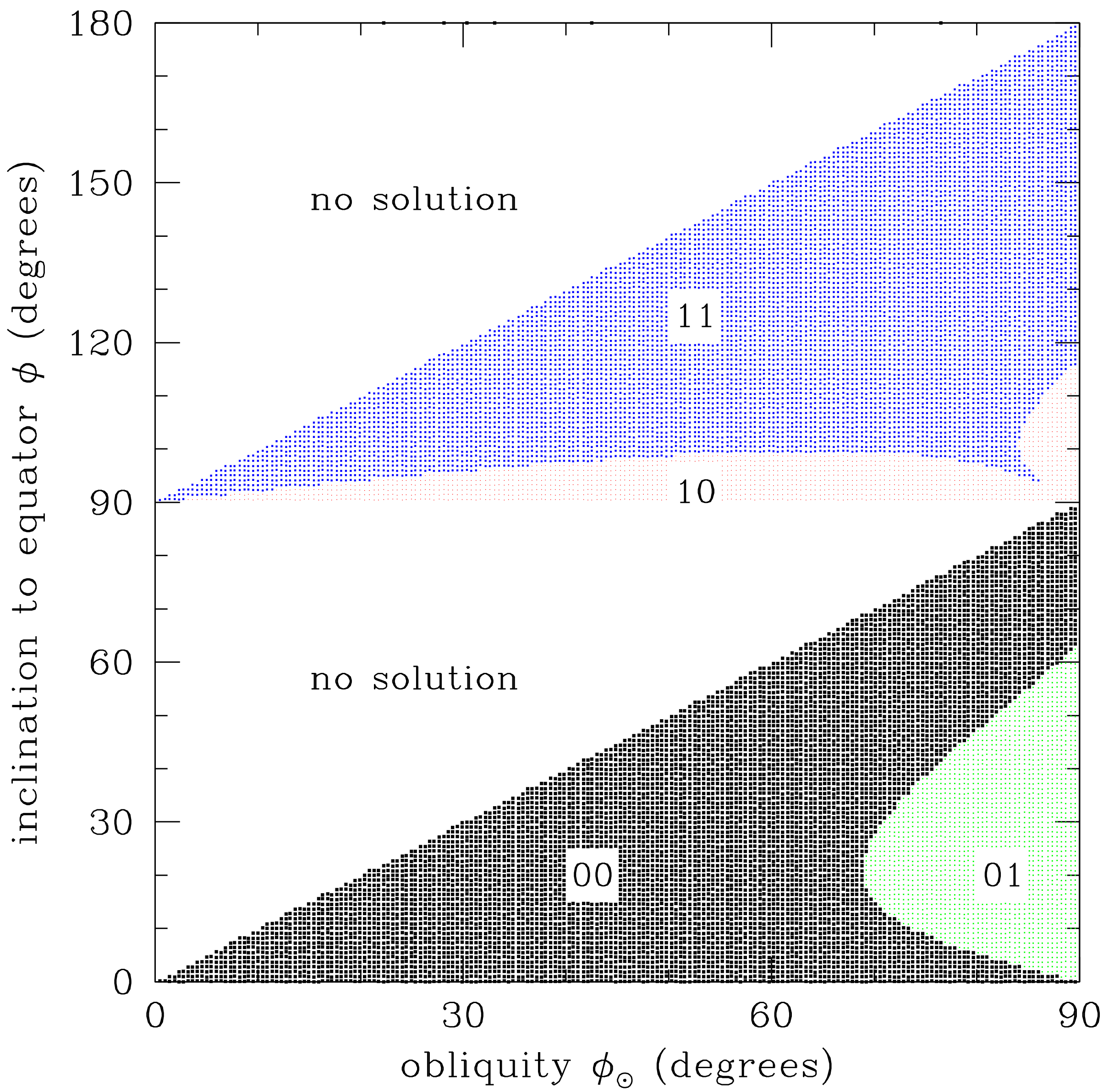

Fig. 1.— The regions in which stable, circular, coplanar Laplace equilibria exist are marked by heavy black stippling and the label "00". In the more lightly stippled regions, circular coplanar equilibria exist but are unstable, according to equations (32) and (34). The first figure in each label is "0" or "1" according to whether the solution is stable or unstable to changes in the orbit plane orientation, described by **j**. The second figure is "0" or "1" according to whether the solution is stable or unstable to changes in the eccentricity, described by **e**. The vertical coordinate is the inclination of the orbit relative to the planetary equator, ϕ. The horizontal coordinate is the obliquity of the planet relative to the ecliptic, $\phi_\odot$. The results are unchanged if $\phi \to \phi + \pi$ or $\phi_\odot \to \phi_\odot + \pi$ or $(\phi_\odot, \phi) \to (\pi - \phi_\odot, \pi - \phi)$.

$$\frac{d\mathbf{e}}{d\tau} \;=\; -\frac{15\epsilon_\odot \mathbf{e}\cdot\mathbf{n}_\odot}{4}\mathbf{j}_0\times\mathbf{n}_\odot + \left(\tfrac{3}{2}\epsilon_\odot - \tfrac{3}{4}\epsilon_p\right)\mathbf{j}_0\times\mathbf{e}. \tag{26}$$

These can be converted to eigenvalue equations by assuming $\mathbf{j}_1, \mathbf{e}_1 \propto \exp(\lambda t)$. To analyze the first equation, set $u = \mathbf{j}_1\cdot\mathbf{n}_\odot$, $v = \mathbf{j}_1\cdot\mathbf{n}_p$. Taking the scalar product of $d\mathbf{j}_1/dt$ with $\mathbf{n}_\odot$ and $\mathbf{n}_p$ we find

$$\frac{du}{d\tau} = \tfrac{3}{2}\epsilon_p\mathbf{n}_\odot\cdot(\mathbf{j}_0\times\mathbf{n}_p)v \quad ; \quad \frac{dv}{d\tau} = \tfrac{3}{4}\epsilon_\odot\mathbf{n}_p\cdot(\mathbf{j}_0\times\mathbf{n}_\odot)u. \tag{27}$$

these can be combined to show that either (i) $u = v = 0$, $\lambda = 0$; this is the unphysical solution noted above; or (ii)

$$\lambda^2 = -\tfrac{9}{8}\epsilon_p\epsilon_\odot[\mathbf{j}_0\cdot(\mathbf{n}_\odot\times\mathbf{n}_p)]^2. \tag{28}$$

since $\lambda^2 < 0$ in this case, $\mathbf{j}_1$ is oscillatory, so the circular orthogonal equilibrium is linearly stable to variations in the angular momentum vector $\mathbf{j}$. The quantity in square brackets is just $\sin\phi_\odot$, where $\phi_\odot$ is the obliquity.

The second of equations (26) can be analyzed similarly. A trivial solution is $\mathbf{e} \propto \mathbf{j}_0$, $\lambda = 0$; this solution is unphysical since the constant of motion $\mathbf{j}\cdot\mathbf{e} = 0$ requires $\mathbf{j}_0\cdot\mathbf{e} = 0$. The other eigenvalues are given by

$$\lambda^2 = \tfrac{9}{16}(3\epsilon_\odot + \epsilon_p)(2\epsilon_\odot - \epsilon_p). \tag{29}$$

Thus the circular orthogonal equilibrium is stable to variations in eccentricity $\mathbf{e}$ if and only if

$$2\epsilon_\odot < \epsilon_p \quad \text{or} \quad a < 2^{-1/5}r_L. \tag{30}$$

3.1.2. The circular coplanar Laplace equilibrium

In the circular coplanar equilibrium, the first of the linearized equations (25) implies that $\mathbf{j}_1 \propto \exp(\lambda t)$ where

$$\lambda^2 = -\tfrac{9}{4}\epsilon_p^2\cos^2\phi - \tfrac{9}{16}\epsilon_\odot^2\cos^2(\phi-\phi_\odot) - \tfrac{9}{16}\epsilon_p\epsilon_\odot[\cos 2\phi + \cos 2(\phi-\phi_\odot) + 2\cos 2\phi_\odot]. \tag{31}$$

Substituting the equilibrium condition (22) we have

$$\lambda^2 = -\frac{9\epsilon_\odot^2}{16}\frac{\sin^2\phi_\odot\cos\phi_\odot}{\sin^2\phi\cos\phi}\cos(\phi-\phi_\odot). \tag{32}$$

The regions in which $\lambda^2 > 0$ (instability) are marked by red and blue stippling and the labels "10" and "11" in Figure 1. All equilibria with $0 < \phi < \frac{1}{2}\pi$ are stable to perturbations of this kind (variations in $\mathbf{j}$ but not $\mathbf{e}$) and equilibria with $\frac{1}{2}\pi < \phi < \pi$ are unstable.

The circular coplanar equilibria that are stable in this sense have $\phi \to 0$ as $a \to 0$ and $\phi \to \phi_\odot$ as $a \to \infty$, so the corresponding Laplace surface coincides with the equator of the planet at small radii and with the planet's orbital plane at large radii. We call this the "classical" Laplace surface since this was the surface discovered by Laplace and the one that has been the focus of most work on this subject.

The second of the linearized equations (25) implies that $\mathbf{e} \propto \exp(\lambda t)$ where

$$\lambda^2 = -\frac{9\epsilon_p^2}{16}[5\cos^4\phi - 2\cos^2\phi + 1] + \frac{9\epsilon_\odot^2}{16}[6 - 7\cos^2(\phi - \phi_\odot)] \\ +\frac{9\epsilon_p\epsilon_\odot}{64}[5 - 6\cos^2\phi - 6\cos^2(\phi - \phi_\odot) - 6\sin 2\phi \sin 2(\phi - \phi_\odot) - 9\cos 2\phi \cos 2(\phi - \phi_\odot)]. \tag{33}$$

Substituting the equilibrium solution (22) we have

$$\begin{aligned}\lambda^2 \;=\; & -\frac{9\epsilon_\odot^2}{2048\sin^2 2\phi}\Big\{ -106 + 24\cos 2\phi + 146\cos 4\phi - 100\cos(6\phi - 2\phi_\odot) \\ & -24\cos(2\phi - 4\phi_\odot) + 224\cos(2\phi - 2\phi_\odot) - 54\cos(4\phi - 4\phi_\odot) - 8\cos 2\phi_\odot - 11\cos 4\phi_\odot \\ & -124\cos(2\phi + 2\phi_\odot) + 25\cos(8\phi - 4\phi_\odot) + 8\cos(4\phi - 2\phi_\odot)\Big\}.\end{aligned} \tag{34}$$

The regions in which $\lambda^2 > 0$ (instability) are marked by green and blue stippling and the labels "01" and "11" in Figure 1.

The inclination to the planetary equator ϕ is plotted as a function of the strength of the planetary quadrupole ϵ_p in Figure 2, for obliquities $\phi_\odot = 10°, 20°, \ldots, 80°$. Solutions for $\phi_\odot > 90°$ can be obtained by the transformation $(\phi, \phi_\odot) \to (\pi - \phi, \pi - \phi_\odot)$.

Unstable equilibria are shown in Figure 2 by dotted or dashed lines. All equilibria with $90° < \phi < 180°$ are unstable. In addition, some of the classical equilibria ($\phi < 90°$) are unstable to eccentricity growth. These are shown as stippled or shaded regions in Figures 3 and 4. Instability first appears at obliquity $\phi_\odot = 68.875°$ and is restricted to semimajor axes between about 0.9 and 1.25 times the Laplace radius r_L (eq. 24).

4. Eccentric Laplace equilibria

We now look for stationary solutions to equations (19) in which the eccentricity $e = |\mathbf{e}|$ is non-zero (recall that $|\mathbf{j}| = (1 - e^2)^{1/2}$). It can be shown (see Appendix C) that all such solutions either have both $\mathbf{j}$ and $\mathbf{e}$ in the principal plane defined by $\mathbf{n}_\odot$ and $\mathbf{n}_p$ (the "coplanar-coplanar" or "eccentric coplanar-coplanar" solution), or one of $\mathbf{j}$ and $\mathbf{e}$ in the principal plane and the other orthogonal to it (the "coplanar-orthogonal" or "orthogonal-coplanar" equilibrium if $\mathbf{j}$ or $\mathbf{e}$, respectively, lies in the principal plane).

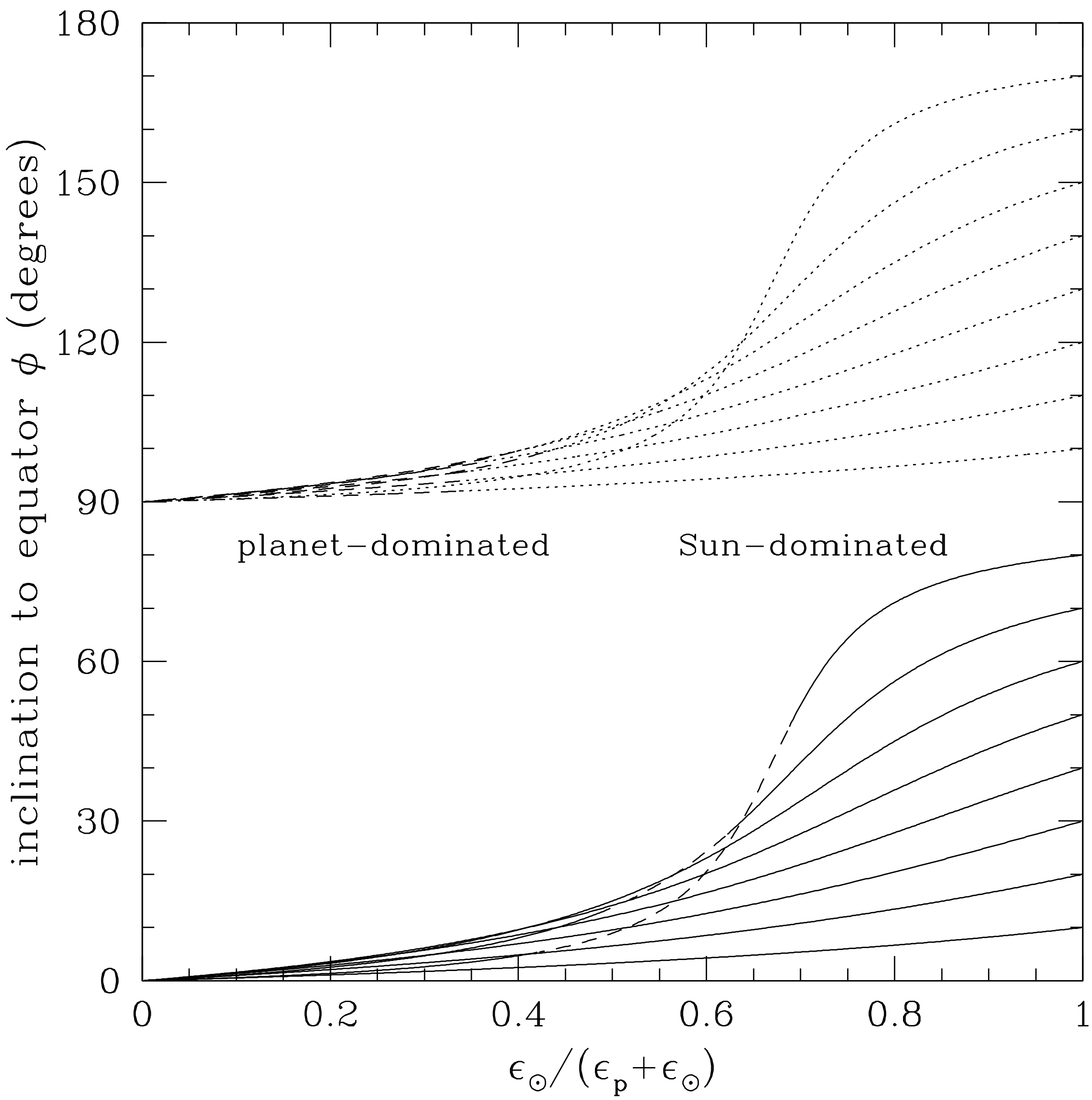

Fig. 2.— Circular coplanar Laplace equilibria. The vertical axis is the angle ϕ between the pole of the planet and the orbital pole of the satellite (the inclination of the orbit relative to the planet's equator). Solutions are shown for eight values of the planetary obliquity, $\phi_\odot = 10°, \ldots, 80°$. There are two equilibrium curves for each obliquity, one with $0 < \phi < 90°$ and the other with $90° < \phi < 180°$. Solid lines denote stable equilibria, while dashed and dotted lines denote equilibria with one or two unstable roots respectively. All equilibria with $\phi > 90°$ are unstable. The classical equilibria are those with $\phi < 90°$. The horizontal axis represents the relative strength of perturbations from the solar tide and the planetary quadrupole (eq. 11); the planetary quadrupole dominates on the left side of the figure and the solar quadrupole on the right.

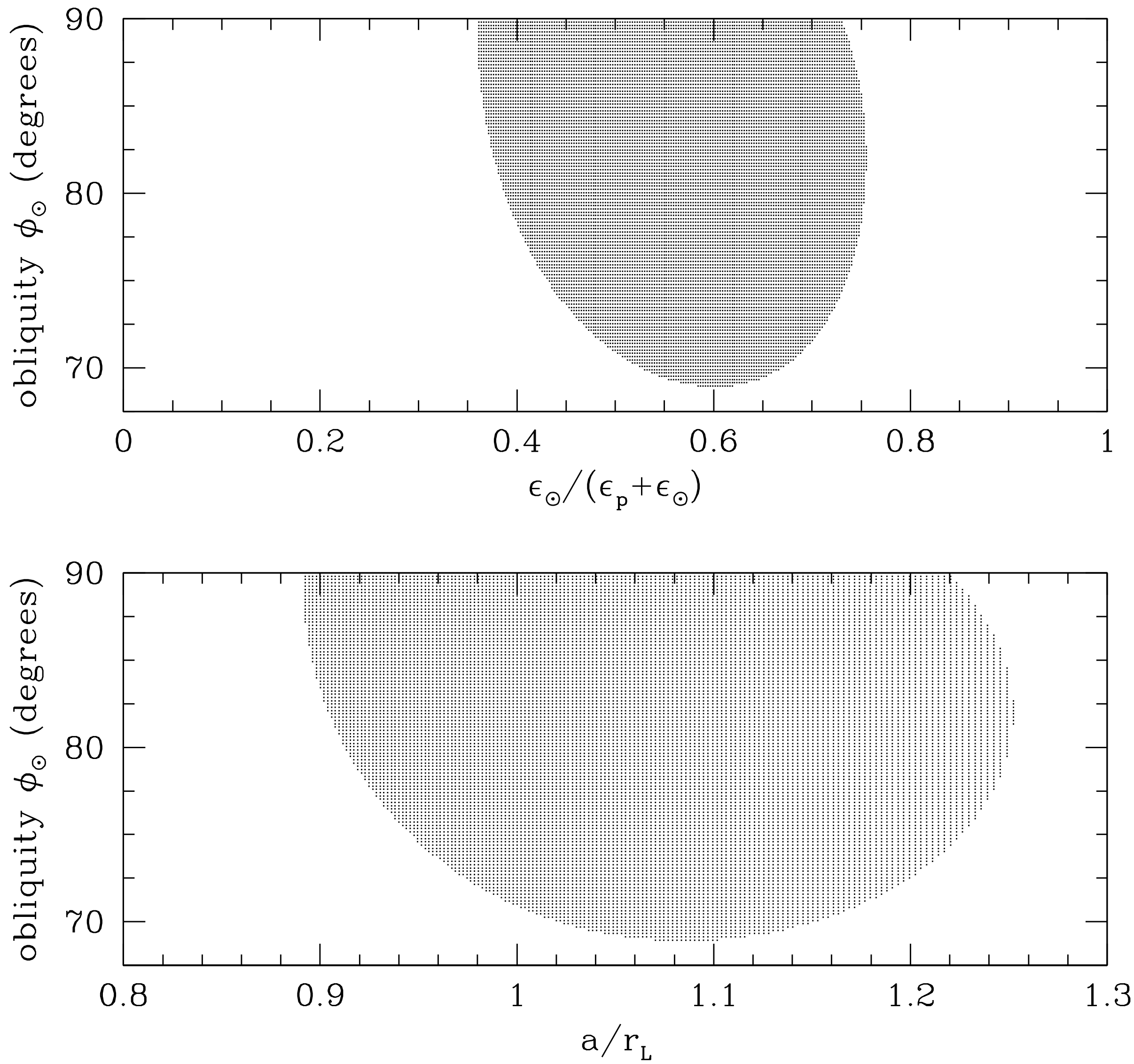

Fig. 3.— Regions in which the classical Laplace equilibria are unstable are stippled. The top panel shows the unstable range of obliquities as a function of the ratio of the solar and planetary perturbation strengths (eq. 11) and the bottom panel shows the unstable obliquities as a function of semimajor axis (in units of the Laplace radius r_L, eq. 24). All instabilities are in the eccentricity vector; the angular-momentum vector is stable.

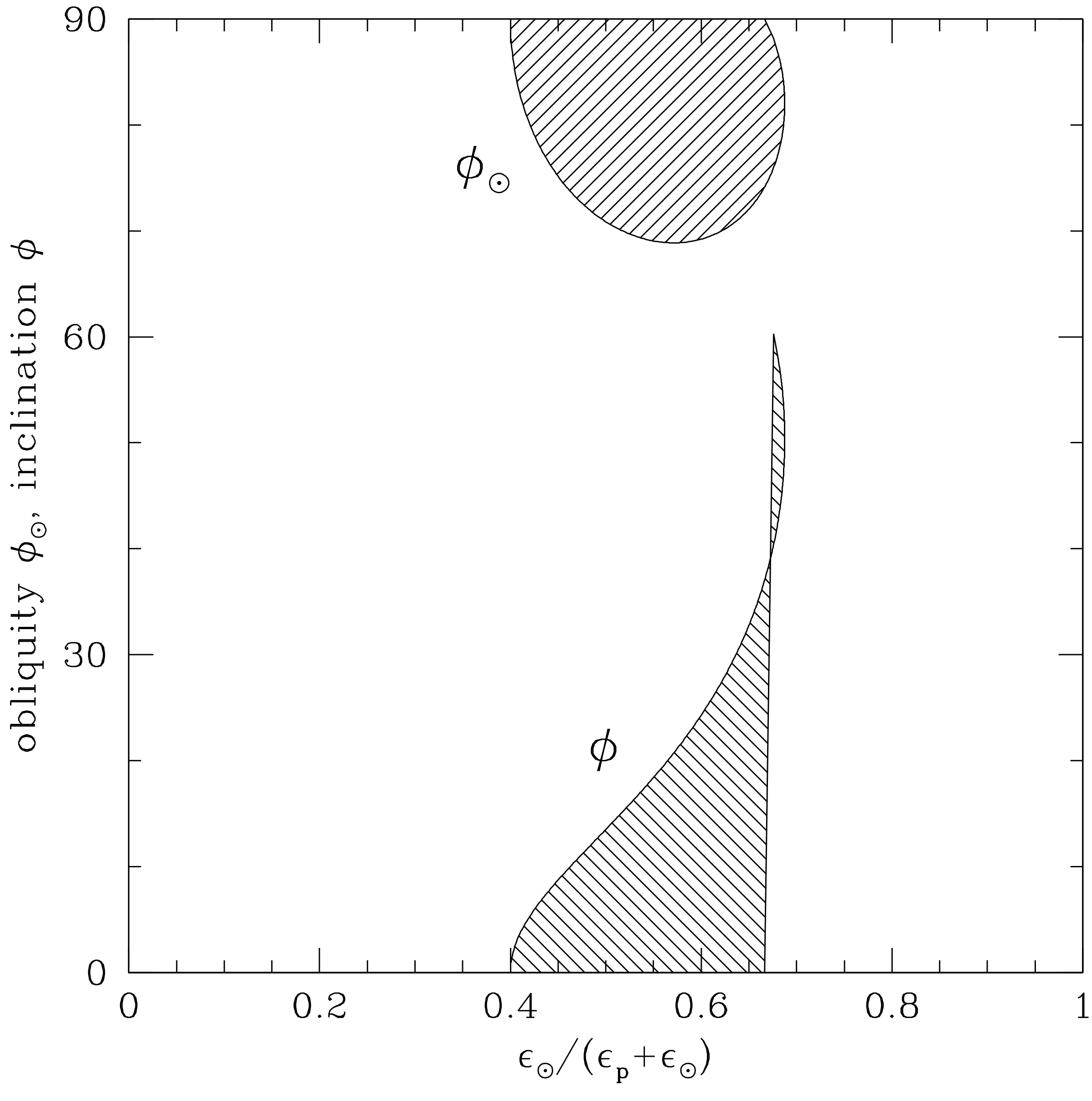

Fig. 4.— Regions in which the classical Laplace equilibria are unstable are shaded.

4.1. Eccentric coplanar-coplanar Laplace equilibrium

In this case $\mathbf{j}$ and $\mathbf{e}$ lie in the principal plane, and equations (19) with $d\mathbf{j}/d\tau = d\mathbf{e}/d\tau = 0$ yield

$$\begin{aligned} 2\epsilon_p \sin 2\phi &= \epsilon_\odot (1-e^2)^{3/2}(1+4e^2)\sin 2(\phi_\odot - \phi) \\ \epsilon_p[1-3\cos^2\phi] &= \epsilon_\odot(1-e^2)^{5/2}[1-4\sin^2(\phi_\odot-\phi)]. \end{aligned} \quad (35)$$

These can be used to solve for e^2 and ϕ, given $\phi_\odot$ and $\epsilon_p/\epsilon_\odot$. The solutions are physical only if $0 < e^2 < 1$.

The regions in $\phi_\odot$–ϕ space in which eccentric coplanar-coplanar Laplace equilibria exist are shown in Figure 5 by stipples. These regions are bounded, in part, by the lines $\phi = \phi_\odot$, $\phi = \phi_\odot + \frac{1}{2}\pi$, and $\phi = \pm\cos^{-1}(1/\sqrt{3}) = 54.7°, 125.3°$. Heavy stippling marks regions in which the equilibria are stable.

The stable regions are small for $\phi > 54.7°$ so we will focus on the region $\phi < 54.7°$. The eccentric coplanar-coplanar equilibria in this region are closely related to the circular coplanar equilibria discussed in §3. We found there that the circular coplanar Laplace equilibria were unstable for a range of $\epsilon_p/\epsilon_\odot$ when the obliquity $\phi_\odot > 68.875°$. Figure 6 shows the range in which the circular coplanar equilibria are stable for $\phi_\odot = 70°, 71°, \ldots, 89°$ as solid horizontal lines, with gaps marking the unstable range. Superimposed on these lines are the eccentric coplanar-coplanar equilibria, marked by heavy blue or light red curves depending on whether they are stable or unstable. The height of these curves is proportional to the eccentricity of the equilibrium. The figure shows that the eccentric coplanar-coplanar equilibria bifurcate from the circular coplanar equilibrium at the point where the circular coplanar equilibrium becomes unstable. The structure of the secular Hamiltonian at the bifurcation is that of the standard resonant Hamiltonian at $j+2:j$ orbital resonances ($k = 2$ in the notation of Borderies & Goldreich 1984).

For $68.875° < \phi_\odot < 71.072°$ the eccentric coplanar-coplanar solution exists in a limited range of $\epsilon_p/\epsilon_\odot$ and is stable throughout this region. For $\phi_\odot > 71.072°$ the eccentric coplanar-coplanar solution is unstable for some part of the range of $\epsilon_p/\epsilon_\odot$ in which it exists. Let us imagine a satellite in the circular coplanar Laplace equilibrium at (say) $\epsilon_\odot/(\epsilon_p+\epsilon_\odot) = 0.8$. If $\epsilon_\odot/(\epsilon_p+\epsilon_\odot)$ slowly decreases (for example, because the satellite is slowly migrating toward the planet) then we expect that (i) for $\phi_\odot < 68.875°$ the satellite will always remain in a circular coplanar Laplace equilibrium; (ii) for $68.875° < \phi_\odot < 71.072°$ the satellite will transfer onto the eccentric coplanar-coplanar equilibrium, its eccentricity will then grow as its spirals in, reach a maximum depending on $\phi_\odot$, then shrink back to zero, at which point it will rejoin the sequence of circular coplanar Laplace equilibria and spiral into the planet on a circular orbit; (iii) for $\phi_\odot > 71.072°$ the satellite will transfer onto the eccentric coplanar-coplanar

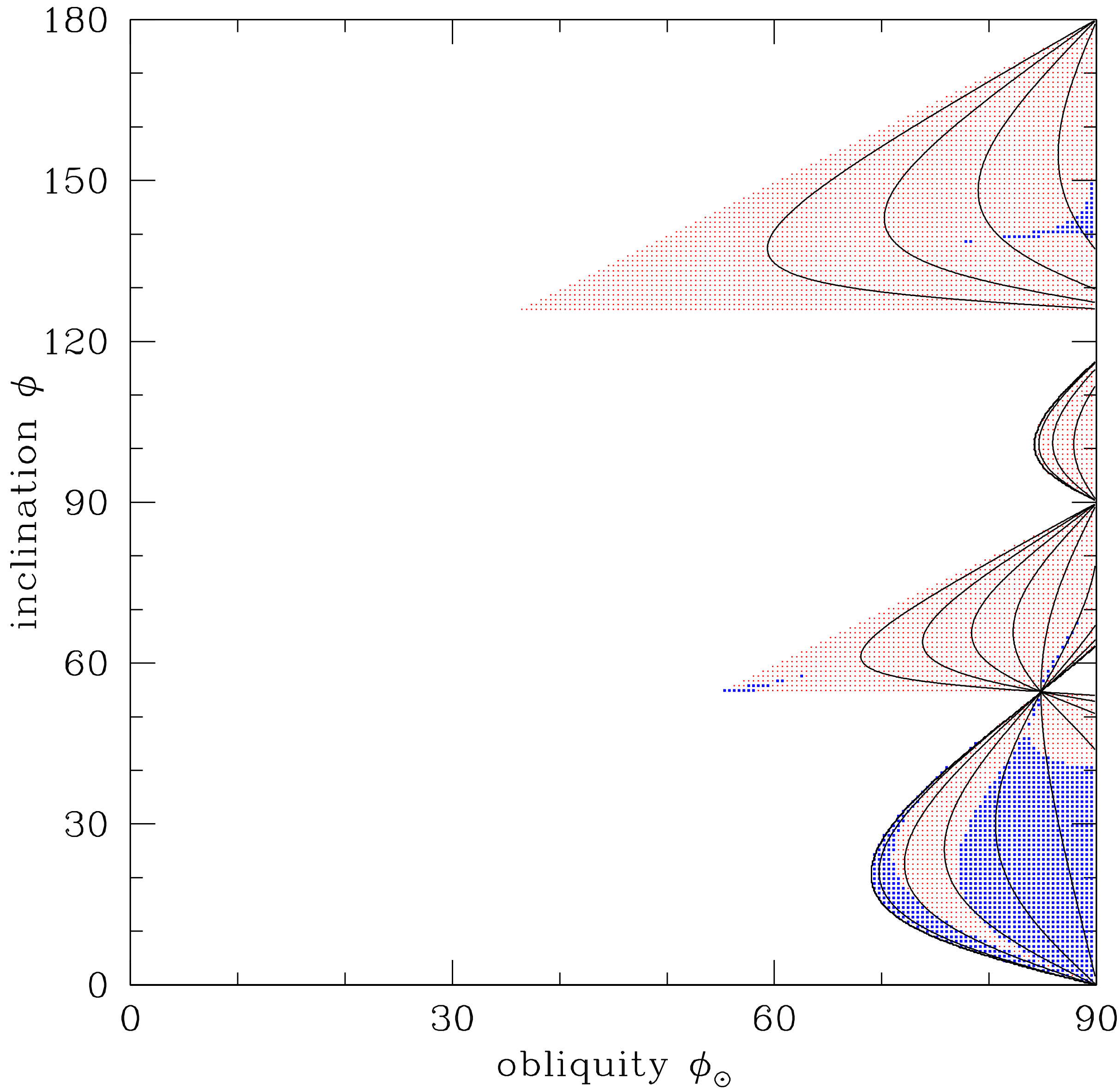

Fig. 5.— Regions in which eccentric coplanar-coplanar Laplace equilibria exist are stippled. Heavy blue and light red stippling mark regions in which the equilibria are respectively stable and unstable. Contours mark eccentricities of $0.1, 0.2, \ldots, 0.9$. Compare to Figure 1.

equilibrium, and its eccentricity will grow until the equilibrium orbit becomes unstable, at which point it presumably undergoes large oscillations in eccentricity and inclination. Numerical simulations of this evolution are described in §5; we shall find that (i) is correct, but that (ii) and (iii) need to be qualified in that orbits track the sequence of eccentric equilibria less well than they imply.

An interesting but difficult question, which we do not attempt to answer here, is the behavior of a dissipative gas or particulate disk in the region where the classical Laplace surface is unstable. There are at least three alternatives: (i) The dissipative forces suppress the secular instabilities in the circular coplanar Laplace equilibria, thereby allowing the disk to occupy the classical Laplace surface. (ii) The disk occupies the surface defined by the eccentric coplanar-coplanar equilibria. A possible problem is the large eccentricity gradients in this sequence of equilibria: a flat, cold disk composed of aligned eccentric orbits cannot exist if $|a(de/da)| > 1$, because the orbits cross. This condition does not apply directly to the Laplace surface because it is not flat; nevertheless, the large eccentricity gradients may lead to strong shears that destabilize the disk. (iii) A gap opens in the disk where the classical Laplace surface is unstable.

4.2. Eccentric coplanar-orthogonal Laplace equilibrium

In this case $\mathbf{j}$ lies in the principal plane and $\mathbf{e}$ is normal to it, so

$$\mathbf{n}_\odot \cdot (\mathbf{j} \times \mathbf{n}_p) = 0, \quad \mathbf{e} \cdot \mathbf{n}_\odot = 0, \quad \mathbf{e} \cdot \mathbf{n}_p = 0.$$

The first of equations (19) with $d\mathbf{j}/d\tau = 0$ yields

$$\epsilon_\odot (1 - e^2)^{5/2} \sin 2(\phi - \phi_\odot) + 2\epsilon_p \sin 2\phi = 0. \tag{36}$$

We introduce a vector $\mathbf{w}$ defined by $\mathbf{w} \times \mathbf{j} = \mathbf{e}$ or $\mathbf{w} = \mathbf{j} \times \mathbf{e}/(1 - e^2)$; $\mathbf{w}$ lies in the principal plane and $\mathbf{w} \cdot \mathbf{j} = \mathbf{w} \cdot \mathbf{e} = 0$. Substituting for $\mathbf{e}$ in the second of equations (19) with $d\mathbf{e}/d\tau = 0$ and $\mathbf{e} \cdot \mathbf{n}_\odot = 0$ yields

$$\begin{aligned} 0 \;=\; & \epsilon_\odot \, \mathbf{j} \cdot \mathbf{n}_\odot [\mathbf{j}(\mathbf{w} \cdot \mathbf{n}_\odot) - \mathbf{w}(\mathbf{j} \cdot \mathbf{n}_\odot)] + \frac{2\epsilon_p \, \mathbf{j} \cdot \mathbf{n}_p}{(1 - e^2)^{5/2}} [\mathbf{j}(\mathbf{w} \cdot \mathbf{n}_p) - \mathbf{w}(\mathbf{j} \cdot \mathbf{n}_p)] \\ & + \left[2\epsilon_\odot - \epsilon_p \frac{1 - e^2 - 5(\mathbf{j} \cdot \mathbf{n}_p)^2}{(1 - e^2)^{7/2}} \right] j^2 \mathbf{w}. \end{aligned} \tag{37}$$

The vectors $\mathbf{j}$ and $\mathbf{w}$ are linearly independent, so the coefficient of each must be zero. The coefficient of $\mathbf{j}$ vanishes if equation (36) is satisfied. The condition that the coefficient of $\mathbf{w}$ vanishes is

$$\epsilon_\odot [2 - \cos^2(\phi_\odot - \phi)] + \frac{\epsilon_p}{(1 - e^2)^{5/2}} (3 \cos^2 \phi - 1) = 0. \tag{38}$$

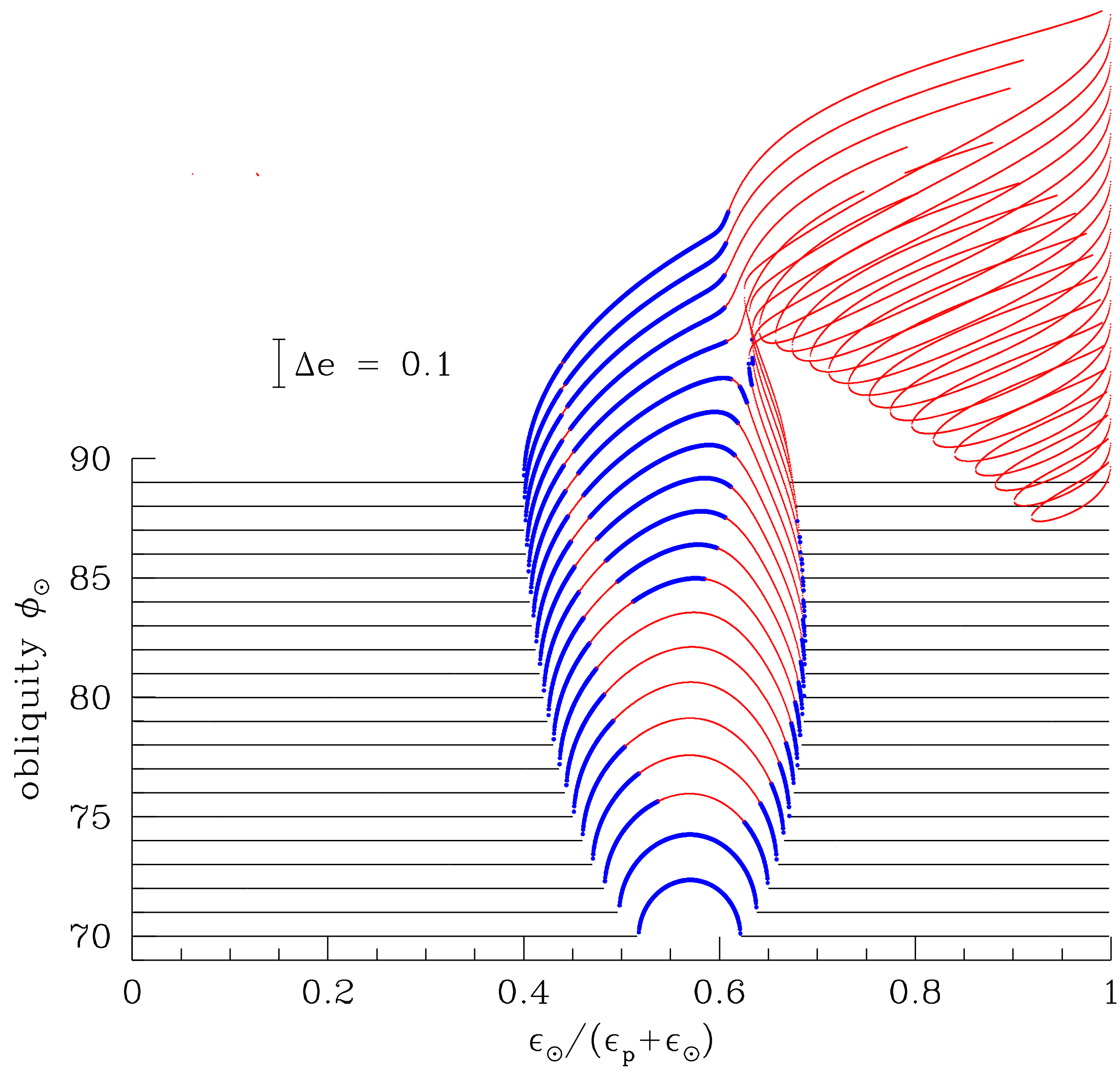

Fig. 6.— The relation of the circular coplanar Laplace equilibria to the eccentric coplanar-coplanar equilibria. The gaps in the solid horizontal lines represent regions in which the circular coplanar equilibria are unstable. The curved lines represent the eccentric coplanar-coplanar Laplace equilibria with inclination $\phi < 90°$. The y-coordinate of these lines is $\phi_\odot + 20e$ where e is the eccentricity of the solution; the curves are heavy blue or light red according to whether the solution is stable or unstable. The figure shows that the eccentric coplanar-coplanar equilibria bifurcate from the circular coplanar equilibria.

Equations (36) and (38) can be combined to eliminate e, $\epsilon_\odot$, and ϵ_p:

$$2[2 - \cos^2(\phi_\odot - \phi)] \sin 2\phi + (3\cos^2\phi - 1) \sin 2(\phi_\odot - \phi) = 0. \tag{39}$$

This result determines the inclination ϕ between the satellite orbit and the planetary spin in terms of the obliquity $\phi_\odot$, independent of ϵ_p, $\epsilon_\odot$, or e. Numerical solution of this equation for $0 \leq \phi_\odot \leq \frac{1}{2}\pi$ shows that there are two solutions for each value of $\phi_\odot$, but the upper solution is unphysical, because these values of ϕ and $\phi_\odot$ yield $\epsilon_\odot(1-e^2)^{5/2}/\epsilon_p < 0$ in equation (36). Thus there is a unique inclination ϕ for each value of the obliquity $\phi_\odot$, as shown in the top panel of Figure 7.

The bottom panel of Figure 7 shows the eccentricity of the coplanar-orthogonal Laplace equilibria. All of these equilibria are unstable.

4.3. Eccentric orthogonal-coplanar Laplace equilibrium

In this case $\mathbf{e}$ lies in the principal plane and $\mathbf{j}$ is normal to it, so

$$\mathbf{j} \cdot \mathbf{n}_p = \mathbf{j} \cdot \mathbf{n}_\odot = 0, \quad \mathbf{e} \cdot (\mathbf{n}_p \times \mathbf{n}_\odot) = 0. \tag{40}$$

The solution of equations (19) with $d\mathbf{j}/d\tau = d\mathbf{e}/d\tau = 0$ requires that

$$\mathbf{e} \cdot \mathbf{n}_\odot = 0, \quad 2\epsilon_\odot(1-e^2)^{5/2} = \epsilon_p. \tag{41}$$

Solutions exist whenever $2\epsilon_\odot > \epsilon_p$.

Linear stability analysis shows that small perturbations in $\mathbf{j}$ or $\mathbf{e}$ grow as $\exp(\lambda t)$ where

$$\lambda^2 = \frac{9\epsilon_\odot^{8/5}\epsilon_p^{2/5}}{2^{12/5}} \sin^2\phi_\odot \quad \text{or} \quad \lambda^2 = \frac{225\epsilon_\odot}{8}\left[1 - (\epsilon_p/2\epsilon_\odot)^{2/5}\right]; \tag{42}$$

since $\lambda^2 < 0$ the eccentric orthogonal-coplanar solutions are stable.

Comparison with the results of §3.1.1 shows that these (eccentric) equilibria bifurcate from the (circular) orthogonal equilibrium sequence at the semimajor axis $a = 2^{-1/5} r_L$ where the latter becomes unstable.

5. Orbital evolution

Consider the evolution of a satellite on a circular orbit that is slowly decaying, so the satellite is migrating toward the planet. Let us assume that the initial semimajor axis is much larger

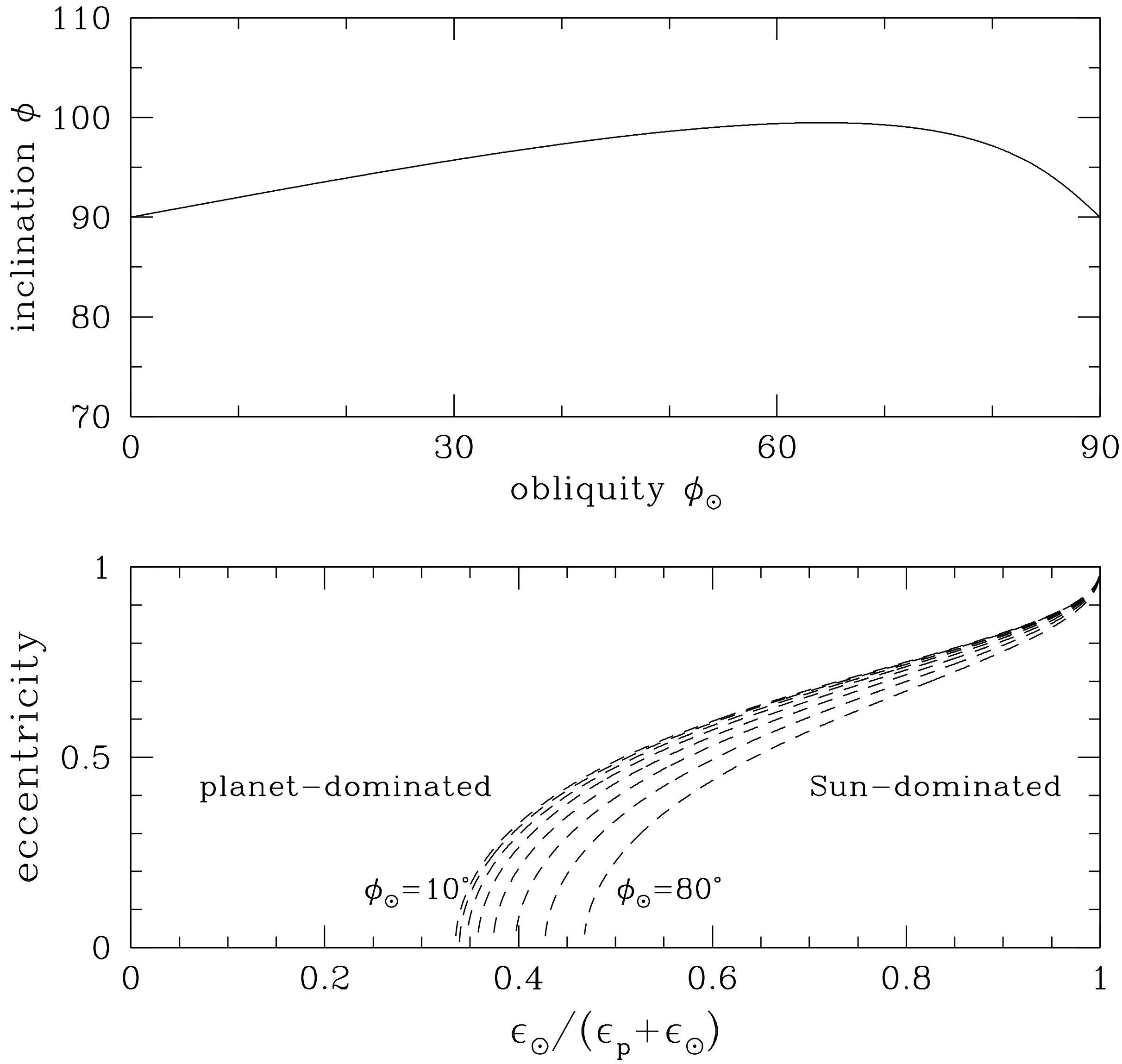

Fig. 7.— (Top) Inclination ϕ as a function of the obliquity $\phi_\odot$ for the eccentric coplanar-orthogonal Laplace equilibrium, as obtained by solving equation (39). (Bottom) Eccentricity of the coplanar-orthogonal equilibrium for obliquity $\phi_\odot = 10, 20, \ldots, 80°$ (left to right). The dashed lines indicate that all of these equilibria have one unstable mode.

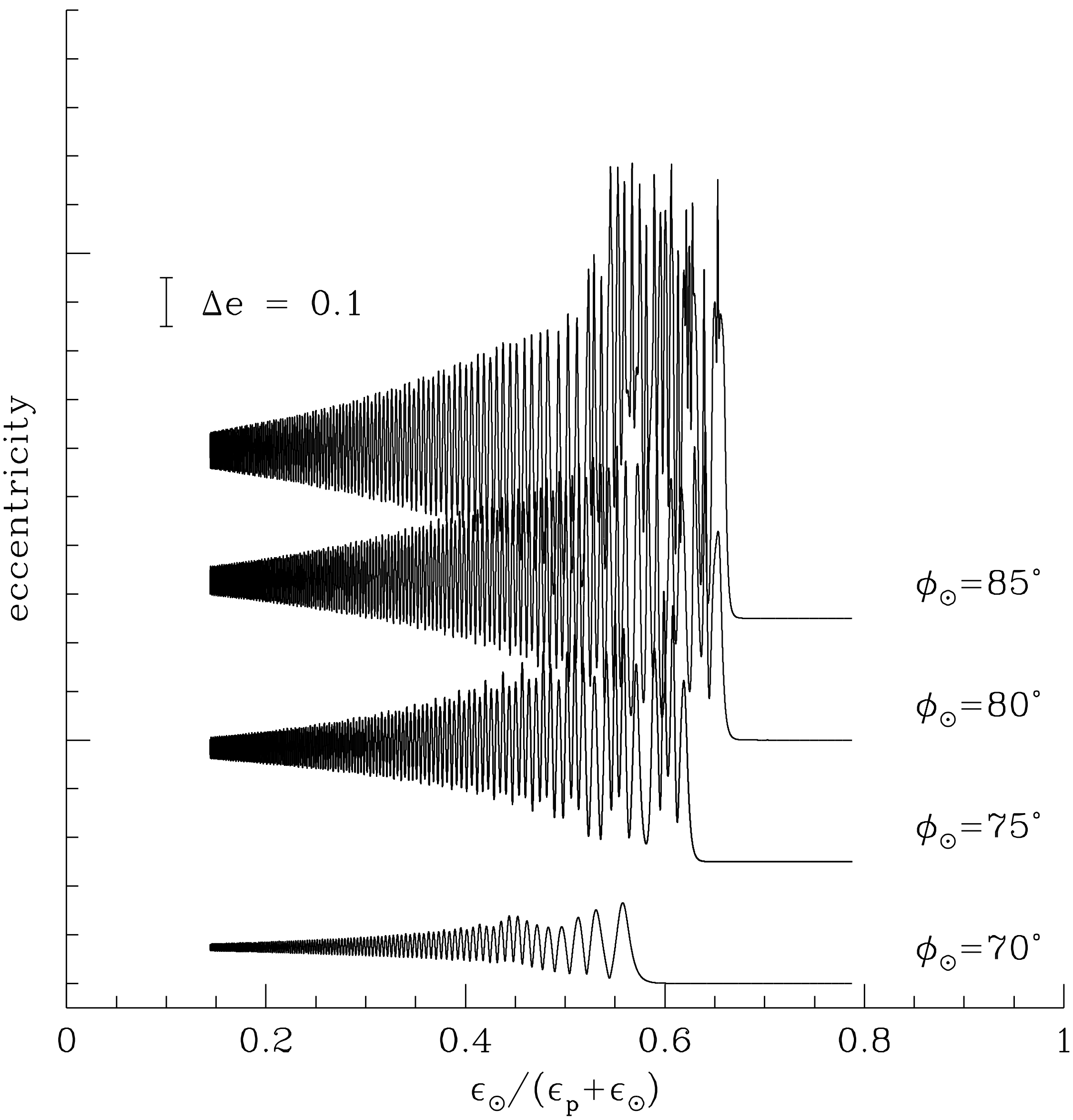

Fig. 8.— Numerical integrations of the equations of motion (19). The y-coordinate is $\phi_\odot+20e$ where e is the eccentricity of the solution. Each orbit is begun at semimajor axis $a = 1.3r_L$ and the semimajor axis then shrinks according to $a/r_L = 1.3 - 0.002\tau$ where τ is defined in equation (11). The satellite is initially in the circular Laplace equilibrium except for a seed eccentricity of 0.0001. The x-coordinate is $\epsilon_\odot/(\epsilon_p + \epsilon_\odot) = a^5/(a^5 + r_L^5)$. Four integrations are shown, for obliquities $\phi_\odot = 70°, 75°, 80°, 85°$.

than the Laplace radius r_L (eq. 24) and that the orbital plane coincides with the planetary orbit (i.e., the satellite is in the classical Laplace surface). As outlined at the end of §4.1, if the obliquity $\phi_\odot < 68.875°$ we expect that the satellite will remain in a circular coplanar Laplace equilibrium as it spirals in. For $68.875° < \phi_\odot < 71.072°$ we expect that at semimajor axis $a \simeq 1.2r_L$ (Fig. 3) the satellite will transfer onto the eccentric coplanar-coplanar equilibrium; its eccentricity will then grow as it migrates inward, reach a maximum depending on $\phi_\odot$, then shrink back to zero, at which point ($a \simeq 0.9r_L$) it will rejoin the classical Laplace surface and spiral into the planet on a circular orbit. Finally, for $\phi_\odot > 71.072°$ the satellite will transfer onto the eccentric coplanar-coplanar equilibrium, and its eccentricity will grow until its orbit becomes unstable and begins to execute large oscillations in eccentricity and inclination

Numerical integrations of the equations of motion (19) are shown for a migrating satellite in Figure 8. As expected, when the initial obliquity $\phi_\odot$ is 75°, 80°, or 85° large eccentricity oscillations develop in the region where the circular coplanar Laplace equilibrium is unstable (compare Fig. 6). Smaller oscillations develop in the case $\phi_\odot = 70°$; these are unexpected since the eccentric coplanar-coplanar sequence is stable at this obliquity, so we would expect smooth growth and decline in the eccentricity as the semimajor axis declines, as in Figure 6. Further integrations show that the behavior of migrating satellites at this obliquity depends on the migration time and other parameters; for example, the orbit shown in Figure 9 follows the eccentric coplanar-coplanar sequence for a while and then rather suddenly jumps to an orbit with a chaotic appearance that reaches eccentricities as high as 0.45. These results suggest the presence of large chaotic regions and perhaps higher order resonances in the phase space, but we have not yet explored these features.

6. Applications

Direct applications of these results to the solar system are rather few. Only Uranus and Pluto have obliquities that exceed the critical value $\phi_\odot = 68.875°$ at which the classical Laplace surface becomes unstable, and these do not have satellites close to the unstable range of semimajor axis.

The circular orthogonal Laplace equilibria have been suggested as possible sites for "polar" rings around Neptune (see Dobrovolskis et al. 1989 and references therein). In this case the solar quadrupole potential is much weaker than the potential from Neptune's satellite Triton. However, the effects of Triton can be modeled approximately using the formalism we have derived, simply replacing the Sun by Triton. We find from equation (24) that the Neptune-Triton Laplace radius is $r_L = 2.15 \times 10^{10}\,\mathrm{cm} = 8.54R_p$. Equation (30) then implies

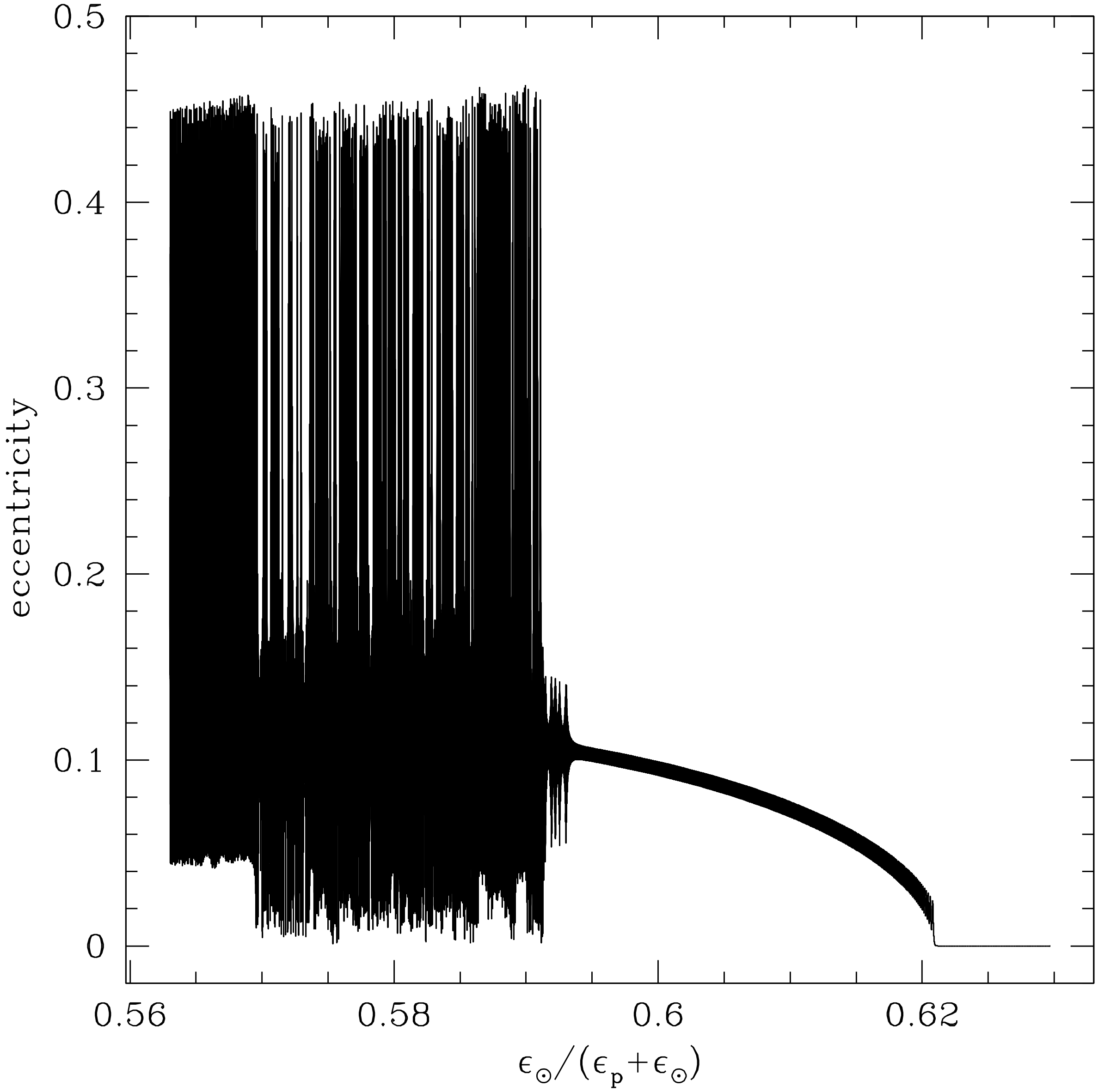

Fig. 9.— Numerical integration of the equations of motion (19) as a satellite migrates inward. The obliquity is $\phi_\odot = 70°$ and the satellite semimajor axis shrinks according to $a/r_L = 1.112 - 0.000002\tau$ where τ is defined in equation (11). The satellite is initially in the circular Laplace equilibrium except for a seed eccentricity of 10^{-6}. The x-coordinate is $\epsilon_\odot/(\epsilon_p + \epsilon_\odot) = a^5/(a^5 + r_L^5)$. The satellite initially lies on the classical Laplace surface; at $\epsilon_\odot/(\epsilon_p + \epsilon_\odot) = 0.621$ it transitions to the eccentric coplanar-coplanar sequence; and at $\epsilon_\odot/(\epsilon_p + \epsilon_\odot) = 0.593$ it transitions to an orbit that exhibits large and irregular eccentricity oscillations.

that circular polar rings would be unstable at semimajor axes $\gtrsim 7.4R_p$, and beyond this radius polar rings must be eccentric. This analysis is only approximate, since (i) the Laplace radius r_L is 61% of Triton's semimajor axis, $a_T = 3.548 \times 10^{10}$ cm, so the approximation of Triton's potential by its quadrupole component is poor; (ii) Triton's orbital axis and Neptune's spin axis both precess around their mutual invariable plane, whereas we have assumed that they are fixed; this is probably only a minor correction, since the precession period of 680 y is much longer than the growth time of the instability, $(a^3/GM_p)^{1/2}/\lambda = 17.3$ y at $a = r_L$; (iii) our calculation neglects collective effects in the ring, such as interparticle collisions, which might suppress the instability.

Our original motivation for examining this problem was the orbit of Saturn's satellite Iapetus, which has an eccentricity of 0.028 and an inclination of 7.5° to the Laplace surface. If it formed from a circumplanetary disk, one might expect Iapetus to have zero eccentricity and inclination relative to this surface. Thus it appears that some process has pumped up Iapetus's inclination while leaving its eccentricity near zero. Ward (1981) pointed out that the shape of the classical Laplace surface is affected by the mass in the circumplanetary disk, and suggested that the current orbit of Iapetus reflects its shape before the disk dispersed. However, this scenario requires the dispersal of the disk in $\lesssim 10^3$ yr—if the dispersal were slower, the inclination relative to the Laplace surface would be an adiabatic invariant and thus would remain near zero. The semimajor axis of Iapetus $a = 59R_p$ is not far from the Laplace radius $r_L = 48R_p$ (Table 1) so it is natural to wonder whether instabilities have excited the inclination. However, (i) at Saturn's obliquity of 26.7°, all circular orbits in the Laplace surface are stable; (ii) the instability we have found in the Laplace surface at high obliquity tends to excite eccentricity, not inclination.

The rich dynamics described in this paper is likely to play a larger role in scenarios in which the obliquities of the giant planets have changed substantially since the formation of the solar system (e.g., Tremaine 1991).

A further application is to extrasolar planetary systems. It is well-known that Kozai oscillations can excite the eccentricity of a single planet orbiting one member of a binary star system (Kozai 1962; Holman et al. 1997; Ford et al. 2000). Now consider a star that hosts two planets, one a hot Jupiter, and belongs to a binary system (see Takeda et al. 2008 for numerical simulations of such systems). The hot Jupiter augments the (otherwise negligible) quadrupole moment of the host star, just as inner satellites augment the quadrupole moment of a planet (eq. 4). The resulting Laplace radius (24) is

$$r_L = 2.7\,\mathrm{AU}\,\left(\frac{m_J}{0.001M_\star}\right)^{1/5}\left(\frac{a_J}{0.1\,\mathrm{AU}}\right)^{2/5}\left(\frac{a_\star}{300\,\mathrm{AU}}\right)^{3/5}(1-e_\star^2)^{3/10}, \qquad (43)$$

where m_J and a_J are the mass and semimajor axis of the hot Jupiter, and $M_\star$, $a_\star$, and $e_\star$

are the mass, semi-major axis, and eccentricity of the binary companion. If, as we expect, the orbital axes of the hot Jupiter and the distant companion star are uncorrelated, 36% of binary stars will have obliquities that exceed the critical value 68.875° at which instabilities set in at some semimajor axis; and if planetary migration is common we expect that many planets now in the habitable zone will have passed through the unstable region and thereby acquired substantial eccentricities (cf. Fig. 8).

7. Summary

We have examined the orbital dynamics of planetary satellites under the combined influence of the quadrupole moment from the planet's equatorial bulge and the tidal field from the Sun. The Laplace equilibria are orbits in which the secular evolution due to these forces is zero. They represent the orbits in which planetary satellites formed from a circumplanetary gas disk should be found.

Laplace equilibria exist for both circular and eccentric orbits. At a given semimajor axis, the orbit normals to the circular Laplace equilibria lie along three orthogonal directions, two of them in the principal plane defined by the planet's spin axis and the normal to its orbit around the Sun (the "circular coplanar" equilibria). One of the two circular coplanar equilibria is always unstable. The warped surface swept out by the other circular coplanar equilibrium orbits as the semimajor axis varies is called the classical Laplace surface (eq. 23). The classical Laplace surface coincides with the equator of the planet at small distances and with the orbital plane of the planet at large distances. Orbits in the classical Laplace surface are stable if the planetary obliquity $\phi_\odot < 68.875°$, while in the range $68.875° < \phi_\odot < 90°$ there is a range of semimajor axes near the Laplace radius r_L (eq. 24) in which the surface is unstable. The third Laplace equilibrium for circular orbits (the "orthogonal" or "polar" equilibrium) corresponds to orbits that cross over the planet's pole, and these are stable if and only if the semimajor axis is less than $2^{-1/5} r_L$ (eq. 30).

At some obliquities and semimajor axes eccentric Laplace equilibria also exist. In the "coplanar-coplanar" equilibria both the eccentricity and angular-momentum vectors lie in the principal plane (Figures 5 and 6). The "orthogonal-coplanar" equilibria are stable, eccentric polar orbits that bifurcate from the circular orthogonal equilibria at the semimajor axis $2^{-1/5} r_L$ where these become unstable. Other eccentric equilibria exist but are unstable.

The use of the secular equations of motion (19) should be legitimate so long as the precession times for the eccentricity and angular-momentum vector are much longer than the orbital period of the satellite. A sufficient condition for this is that the satellite semi-

major axis is much larger than the planetary radius and much smaller than the planet's Hill radius (cf. Table 1). A possible limitation of the secular equations is that they neglect the evection resonance, where the apsidal precession rate equals the mean motion of the planet around the Sun. For the outer planets, the evection resonance typically occurs at $\sim 0.2 r_L$. Touma & Wisdom (1998) have stressed the role of the evection resonance in the history of the lunar orbit.

Several unanswered questions remain: (i) What is the structure of the four-dimensional phase space of the equations of motion (19), and what fraction of the orbits are chaotic? These issues could be explored through surfaces of section, although the exploration would be laborious since there is a separate surface of section for each value of the Hamiltonian, semimajor axis, and planetary obliquity. (ii) What is the nature of the evolution of satellites in the classical Laplace surface that migrate into an unstable region (Fig. 8)? (iii) What are the shape and properties of dissipative disks in the range of semimajor axes where the classical Laplace surface is unstable? Does the dissipation stabilize the classical Laplace surface? Does the disk follow the eccentric coplanar-coplanar Laplace surface? Or is there no steady-state disk? Hints that eccentric structures can occur in dissipative disks include the eccentric structures seen in the planetary ring systems of Uranus and Saturn, debris disks around young stars, and galactic nuclei such as M31. (iv) What is the analog of the Laplace surface in accretion disks around black holes, where Lense–Thirring precession rather than a quadrupole potential is the dominant non-Keplerian perturbation from the central body?

We thank Yuri Levin for thoughtful comments. This research was supported in part by NASA grants NNX08AH83G and NNX08AH24G, and by NSF grant AST-0807432.

A. Gauge dependence in the averaged potential

The orbit-averaged potential $\Psi(\mathbf{j}, \mathbf{e})$ is a function of the six scalar components of $\mathbf{j}$ and $\mathbf{e}$ but is only physically meaningful on the four-dimensional manifold defined by the constraints (17). Thus Ψ may be replaced by $\Psi + F$, where the gauge function $F(\mathbf{j}, \mathbf{e})$ is arbitrary except that $F = \text{const}$ on the manifold (17). We now show that $F(\mathbf{j}, \mathbf{e})$ has no effect on the equations of motion (18), just as adding a constant to a Newtonian potential ϕ has no effect on the equations of motion $\ddot{\mathbf{x}} = -\boldsymbol{\nabla}\phi$.

We work in the coordinates with axes parallel to the unit vectors $(\mathbf{u}, \mathbf{v}, \mathbf{n})$ defined just before equation (7). Substituting F for Ψ in the equations of motion (18) and observing

that $\mathbf{j} = j\mathbf{n}$, $\mathbf{e} = e\mathbf{u}$, we have

$$\begin{aligned}
\frac{d\mathbf{j}}{d\tau} &= -j\mathbf{v}(\boldsymbol{\nabla}_\mathbf{j}F\cdot\mathbf{u}) + j\mathbf{u}(\boldsymbol{\nabla}_\mathbf{j}F\cdot\mathbf{v}) - e\mathbf{n}(\boldsymbol{\nabla}_\mathbf{e}F\cdot\mathbf{v}) + e\mathbf{v}(\boldsymbol{\nabla}_\mathbf{e}F\cdot\mathbf{n})\\
\frac{d\mathbf{e}}{d\tau} &= -j\mathbf{v}(\boldsymbol{\nabla}_\mathbf{e}F\cdot\mathbf{u}) + j\mathbf{u}(\boldsymbol{\nabla}_\mathbf{e}F\cdot\mathbf{v}) - e\mathbf{n}(\boldsymbol{\nabla}_\mathbf{j}F\cdot\mathbf{v}) + e\mathbf{v}(\boldsymbol{\nabla}_\mathbf{j}F\cdot\mathbf{n}).
\end{aligned} \tag{A1}$$

The gauge condition that $F = \text{const}$ on the manifold (17) is

$$0 = dF = \boldsymbol{\nabla}_\mathbf{j}F\cdot d\mathbf{j} + \boldsymbol{\nabla}_\mathbf{e}F\cdot d\mathbf{e} \quad \text{when} \quad \mathbf{e}\cdot d\mathbf{j} + \mathbf{j}\cdot d\mathbf{e} = 0 \text{ and } \mathbf{j}\cdot d\mathbf{j} + \mathbf{e}\cdot d\mathbf{e} = 0. \tag{A2}$$

We write $d\mathbf{j}$ and $d\mathbf{e}$ in terms of the unit vectors $(\mathbf{u}, \mathbf{v}, \mathbf{n})$ as

$$d\mathbf{j} = a_u\mathbf{u} + a_v\mathbf{v} + a_n\mathbf{n}, \qquad d\mathbf{e} = b_u\mathbf{u} + b_v\mathbf{v} + b_n\mathbf{n}; \tag{A3}$$

then (A2) requires that

$$0 = a_u(\boldsymbol{\nabla}_\mathbf{j}F\cdot\mathbf{u}) + a_v(\boldsymbol{\nabla}_\mathbf{j}F\cdot\mathbf{v}) + a_n(\boldsymbol{\nabla}_\mathbf{j}F\cdot\mathbf{n}) + b_u(\boldsymbol{\nabla}_\mathbf{e}F\cdot\mathbf{u}) + b_v(\boldsymbol{\nabla}_\mathbf{e}F\cdot\mathbf{v}) + b_n(\boldsymbol{\nabla}_\mathbf{e}F\cdot\mathbf{n}) \tag{A4}$$

when

$$ea_u + jb_n = 0, \quad ja_n + eb_u = 0. \tag{A5}$$

The six variables $a_u, a_v, a_n, b_u, b_v, b_n$ can be chosen arbitrarily so long as they satisfy the two constraints (A5). Thus (A4) can only be true if the gauge function F satisfies four conditions:

$$\boldsymbol{\nabla}_\mathbf{j}F\cdot\mathbf{v} = 0, \quad \boldsymbol{\nabla}_\mathbf{e}F\cdot\mathbf{v} = 0, \quad j\boldsymbol{\nabla}_\mathbf{j}F\cdot\mathbf{u} = e\boldsymbol{\nabla}_\mathbf{e}F\cdot\mathbf{n}, \quad e\boldsymbol{\nabla}_\mathbf{j}F\cdot\mathbf{n} = j\boldsymbol{\nabla}_\mathbf{e}F\cdot\mathbf{u}. \tag{A6}$$

With these conditions, equations (A1) yield $d\mathbf{j}/d\tau = 0$, $d\mathbf{e}/d\tau = 0$, so the gauge function has no effect on the equations of motion.

B. Behavior of circular orbits

A circular orbit remains circular under the perturbations in question; that is, there is a set of solutions of equations (19) in which $\mathbf{e} = 0$ for all time. The dynamics of the circular orbit is governed by the three-dimensional system of equations

$$\frac{d\mathbf{j}}{d\tau} = \frac{3\epsilon_\odot\,\mathbf{j}\cdot\mathbf{n}_\odot}{4}\mathbf{j}\times\mathbf{n}_\odot + \frac{3\epsilon_p\mathbf{j}\cdot\mathbf{n}_p}{2}\mathbf{j}\times\mathbf{n}_p. \tag{B1}$$

This system has two integrals of motion, $|\mathbf{j}|$ (equal to unity on the manifold corresponding to physical solutions) and the associated Hamiltonian (eq. 10, for $e = 0$). The system is

integrable, as we now demonstrate by recasting the problem in the form of free rigid-body dynamics with the appropriate inertia tensor.

First, note that $(\mathbf{j}\cdot\mathbf{n}_\odot)\,\mathbf{j}\times\mathbf{n}_\odot = \mathbf{j}\times(\mathbf{j}\cdot\mathbf{n}_\odot)\mathbf{n}_\odot$ can be rewritten in the form $\mathbf{j}\times\mathbf{T}_\odot\cdot\mathbf{j}$ where

$$\mathbf{T}_\odot = \left(\begin{array}{lll} n_1^2 & n_1n_2 & n_1n_3 \\ n_2n_1 & n_2^2 & n_2n_3 \\ n_3n_1 & n_3n_2 & n_3^2 \end{array}\right)_\odot \tag{B2}$$

is a symmetric tensor built out of the components of $\mathbf{n}_\odot = (n_1, n_2, n_3)_\odot$. The same can be done for the $\mathbf{n}_p$ term leading to an equivalent symmetric tensor $\mathbf{T}_p$, built out of the components of $\mathbf{n}_p$. We can thus rewrite equation (B1) in the suggestive form

$$\frac{d\mathbf{j}}{d\tau} = \mathbf{j}\times\mathbf{T}\cdot\mathbf{j} \quad \text{where} \quad \mathbf{T} = \alpha\mathbf{T}_\odot + \beta\mathbf{T}_p, \tag{B3}$$

with $\alpha = \frac{3}{4}\epsilon_\odot$ and $\beta = \frac{3}{2}\epsilon_p$. Following this rearrangement, the program is straightforward: we find the matrix that diagonalizes the symmetric tensor $\mathbf{T}$, identifying principal directions (actually the directions of the circular Laplace equilibria discussed in §3), and the principal values, which will decide the stability of equilibria and the global phase-space topology around them. To fix things, it is simplest to take $\mathbf{n}_p = (1, 0, 0)$, and $\mathbf{n}_p = (\cos\phi_\odot, \sin\phi_\odot, 0)$ (obliquity $\phi_\odot$), leading to:

$$\mathbf{T} = \left(\begin{array}{lll} \alpha\cos^2\phi_\odot + \beta & \alpha\cos\phi_\odot\sin\phi_\odot & 0 \\ \alpha\cos\phi_\odot\sin\phi_\odot & \alpha\sin^2\phi_\odot & 0 \\ 0 & 0 & 0 \end{array}\right). \tag{B4}$$

The eigenvalues of $\mathbf{T}$ are

$$\begin{aligned} t_1 &= 0 \\ t_2 &= \frac{\alpha+\beta-\sqrt{(\alpha+\beta)^2-4\alpha\beta\,\sin^2\phi_\odot}}{2} \\ t_3 &= \frac{\alpha+\beta+\sqrt{(\alpha+\beta)^2-4\alpha\beta\,\sin^2\phi_\odot}}{2}, \end{aligned} \tag{B5}$$

with $t_1 = 0 < t_2 < t_3$ ($t_2 = 0$ for $\phi_\odot = 0$, an ignorable case). We can then solve for the eigenvectors $\mathbf{t}^{(1)}$, $\mathbf{t}^{(2)}$, $\mathbf{t}^{(3)}$ of $\mathbf{T}$, the principal axis directions. Since $\mathbf{T}$ is symmetric its eigenvectors are orthogonal. Moreover the eigenvectors can be chosen to be orthonormal and to form a right-handed triad ($\mathbf{t}^{(1)} = \mathbf{t}^{(2)}\times\mathbf{t}^{(3)}$). In particular, $\mathbf{t}^{(1)} = (0, 0, \pm1)$ (assuming, as usual, that ϵ_p, $\epsilon_\odot$, and $\sin\phi_\odot$ are non-zero), that is, $\mathbf{t}^{(1)}$ is perpendicular to the principal plane containing $\mathbf{n}_p$ and $\mathbf{n}_\odot$, while $\mathbf{t}^{(2)}$ and $\mathbf{t}^{(3)}$ lie in the principal plane.

Let $\mathbf{R}$ be the orthogonal transformation associated with these vectors, the transformation that diagonalizes $\mathbf{T}$. The columns of $\mathbf{R}$ are the orthonormal eigenvectors of $\mathbf{T}$, so

$R_{ij} = t_i^{(j)}$. We now rotate to the principal-axis coordinate system, by setting $\mathbf{j} = \mathbf{R} \cdot \mathbf{J}$. Equation (B3) turns into

$$\begin{aligned}\frac{dJ_1}{dt} &= (t_3 - t_2) J_2 J_3 \\ \frac{dJ_2}{dt} &= (t_1 - t_3) J_1 J_3 = -t_3 J_1 J_3 \\ \frac{dJ_3}{dt} &= (t_2 - t_1) J_1 J_2 = t_2 J_1 J_2,\end{aligned} \tag{B6}$$

exactly what one would obtain for the asymmetrical top in Euler's formulation, with $1/t_i$ standing for I_i, the principal moments of inertia (Landau & Lifshitz 1976). As in the case of the rigid body, vectors that lie along the principal axes (parallel and anti-parallel) are stationary states of the dynamics: $\mathbf{J} = (\pm 1, 0, 0)$, $(0, \pm 1, 0)$, and $(0, 0, \pm 1)$.

The equilibria along $\mathbf{t}^{(1)}$ are linearly stable, with linear oscillation frequency $\Omega_1 = \sqrt{t_2\, t_3}$ (t_2 and t_3 are both positive); equilibria along $\mathbf{t}^{(3)}$ are also stable, with linear oscillation frequency $\Omega_2 = \sqrt{(t_3 - t_2)\, t_3}$ ($t_3 > t_2 > 0$); equilibria along $\mathbf{t}^{(2)}$ are linearly unstable with growth rate $\sqrt{t_2(t_3 - t_2)}$. Thus $\mathbf{t}^{(3)}$ and $\mathbf{t}^{(2)}$ describe the directions of the angular-momentum vectors for the linearly stable and unstable circular coplanar Laplace equilibria, while $\mathbf{t}^{(1)}$ describes the circular orthogonal Laplace equilibrium, which is stable (recall that we consider only circular orbits in this Appendix, so the stability properties described here do not include the eccentricity instabilities discussed in §3.1).

We now examine the nonlinear dynamics. The Hamiltonian is the restriction of $\Psi_p + \Psi_\odot$ (eq. 12) to circular orbits, $e = 0$. In the present notation this can be written

$$H_c = -\tfrac{1}{2}\mathbf{j}^{\mathrm{T}} \cdot \mathbf{T} \cdot \mathbf{j} = -\tfrac{1}{2} \sum_{i=1}^{3} t_i J_i^2 = -\tfrac{1}{2}(t_2 J_2^2 + t_3 J_3^2), \tag{B7}$$

where the superscript "T" denotes transpose. If it is not clear already, note that H_c generates Lie-Poisson dynamics of $\mathbf{J}$ according to:

$$\frac{d\mathbf{J}}{d\tau} = -\mathbf{J} \times \boldsymbol{\nabla}_{\mathbf{J}} H_c. \tag{B8}$$

There are two integrals of motion, H_c itself and the magnitude $J^2 = J_1^2 + J_2^2 + J_3^2 = 1$. Thus trajectories lie on the intersection of the angular momentum sphere and the elliptical cylinder representing the energy surface (as opposed to the ellipsoid with axes $1/I_i$ that is involved in the solution of the asymmetrical top). The largest allowable energy is $H_{c,\max} = 0$ and the smallest is $H_{c,\min} = -\frac{1}{2}t_3$. Starting at the minimum energy, the cylinder intersects the sphere at two points, corresponding to equilibria along $\mathbf{t}^{(3)}$. Increasing the energy, the

cylinder intersects the sphere in closed curves around these equilibria. This remains so, till we reach the critical energy $H_c = -\frac{1}{2}t_2$, at which point the cylinder is tangent to the sphere at $\pm\mathbf{t}^{(2)}$ as it intersects it along the limiting curves, separatrices, that separate the stable librations around $\mathbf{t}^{(3)}$ from the stable librations around $\mathbf{t}^{(1)}$. Increasing further, the cylinder now intersects the sphere at two librating curves around $\pm\mathbf{t}^{(1)}$, until it reduces to a needle piercing the sphere at $\pm\mathbf{t}^{(1)}$ when $H_c = 0$.

Orbit shapes are easy to obtain in projection. For trajectories librating around the $\mathbf{t}^{(3)}$ equilibrium, take the ratio of the J_1 and J_2 equations and integrate (or eliminate J_3^2 between the energy and angular-momentum integrals) to get

$$(t_3 - t_2)J_2^2 + t_3 J_1^2 = \text{const} = t_3 + 2H_c, \qquad -t_3 \leq 2H_c < -t_2. \tag{B9}$$

At the limiting value, $H_c = -\frac{1}{2}t_2$, this defines the separatrices in projection. Similarly we can obtain trajectories librating around the $\mathbf{t}^{(1)}$ equilibrium. Of course the equations of motion (B6) can be solved explicitly, following the methods used for the asymmetrical top (Landau & Lifshitz 1976).

Incidentally, if the system is subject to a process that dissipates energy while conserving angular momentum, it will decay towards the minimum energy state, which lies along $\pm\mathbf{t}^{(3)}$, the direction normal to the circular coplanar Laplace equilibrium. This is often interpreted to mean that the classical Laplace surface, at a minimum of H_c, is secularly stable while the circular orthogonal Laplace equilibrium at a maximum of H_c is secularly unstable. However, most dissipative processes also affect the eccentricity and semimajor axes of the orbits, so the evolution of the orientation of the angular-momentum vector due to dissipation cannot be treated in isolation. In particular, Dobrovolskis et al. (1989) argue in the context of possible polar rings around Neptune that the circular orthogonal Laplace equilibria are secularly stable.

C. Classification of eccentric Laplace equilibria

We investigate the properties of Laplace equilibria (stationary solutions of eqs. 19) with non-zero eccentricity. As usual we assume that $\epsilon_p > 0$ and that $\mathbf{n}_\odot$ is neither parallel, antiparallel, nor perpendicular to $\mathbf{n}_p$. Recall that $|\mathbf{j}| = (1 - e^2)^{1/2}$.

Take the scalar product of the first of equations (19) with $\mathbf{n}_\odot$. The first two terms on the right side vanish, and since $d\mathbf{j}/d\tau = 0$ in a stationary solution and $\epsilon_p \neq 0$ we must have either

$$\text{(a) } \mathbf{n}_\odot \cdot (\mathbf{j} \times \mathbf{n}_p) = 0, \qquad \text{or} \qquad \text{(b) } \mathbf{j} \cdot \mathbf{n}_p = 0. \tag{C1}$$

First consider case (a). Take the scalar product of the second of equations (19) with $\mathbf{e}$. The first, third, and fourth terms on the right side vanish, and $\epsilon_\odot \neq 0$, so we must have either

$$\begin{aligned} &\text{(aa) } \mathbf{n}_\odot \cdot (\mathbf{j} \times \mathbf{n}_p) = 0 \qquad \text{and} \qquad \mathbf{e} \cdot (\mathbf{j} \times \mathbf{n}_\odot) = 0, \qquad \text{or} \\ &\text{(ab) } \mathbf{n}_\odot \cdot (\mathbf{j} \times \mathbf{n}_p) = 0 \qquad \text{and} \qquad \mathbf{e} \cdot \mathbf{n}_\odot = 0. \end{aligned} \tag{C2}$$

Case (aa) requires that $\mathbf{j}$, $\mathbf{e}$, $\mathbf{n}_\odot$, and $\mathbf{n}_p$ are all coplanar, that is, that $\mathbf{j}$ and $\mathbf{e}$ lie in the principal plane defined by $\mathbf{n}_\odot$ and $\mathbf{n}_p$. We call this the "coplanar-coplanar" solution since $\mathbf{j}$ and $\mathbf{e}$ lie in the principal plane. Case (ab) requires that $\mathbf{j}$, $\mathbf{n}_\odot$, and $\mathbf{n}_p$ are coplanar and that $\mathbf{e}$ is perpendicular to $\mathbf{n}_\odot$; moreover by definition $\mathbf{e}$ is perpendicular to $\mathbf{j}$. Hence $\mathbf{j}$ lies in the principal plane and $\mathbf{e}$ is normal to this plane; we call this the "coplanar-orthogonal" solution.

Now consider case (b). Take the scalar product of the first of equations (19) with $\mathbf{e}$. The second and third terms on the right side vanish, so either

$$\begin{aligned} &\text{(ba) } \mathbf{j} \cdot \mathbf{n}_p = 0 \qquad \text{and} \qquad \mathbf{j} \cdot \mathbf{n}_\odot = 0, \quad \text{or} \\ &\text{(bb) } \mathbf{j} \cdot \mathbf{n}_p = 0 \qquad \text{and} \qquad \mathbf{e} \cdot (\mathbf{j} \times \mathbf{n}_\odot) = 0. \end{aligned} \tag{C3}$$

In case (ba), the first of equations (19) implies that $(\mathbf{e} \cdot \mathbf{n}_\odot)\mathbf{e} \times \mathbf{n}_\odot = 0$. Hence either

$$\begin{aligned} &\text{(baa) } \mathbf{j} \cdot \mathbf{n}_p = 0 \qquad \text{and} \qquad \mathbf{j} \cdot \mathbf{n}_\odot = 0 \quad \text{and} \quad \mathbf{e} \cdot \mathbf{n}_\odot = 0, \quad \text{or} \\ &\text{(bab) } \mathbf{j} \cdot \mathbf{n}_p = 0 \qquad \text{and} \qquad \mathbf{j} \cdot \mathbf{n}_\odot = 0 \quad \text{and} \quad \mathbf{e} \times \mathbf{n}_\odot = 0. \end{aligned} \tag{C4}$$

In case (baa), $\mathbf{j}$ is perpendicular to the principal plane, and $\mathbf{e}$ lies in the principal plane at right angles to $\mathbf{n}_\odot$; we call this the "orthogonal-coplanar" solution. In case (bab) $\mathbf{e}$ is parallel or antiparallel to $\mathbf{n}_\odot$ so we can write $\mathbf{e} = \pm e\mathbf{n}_\odot$ and the second of equations (19) reduces to

$$3\epsilon_\odot + \frac{\epsilon_p}{(1-e^2)^{5/2}} = 0, \tag{C5}$$

which has no solution since $\epsilon_\odot, \epsilon_p > 0$.

In case (bb), $\mathbf{e}$, $\mathbf{j}$, and $\mathbf{n}_\odot$ lie in the same plane, and the first of equations (19) reduces to

$$(\mathbf{j} \cdot \mathbf{n}_\odot)\mathbf{j} \times \mathbf{n}_\odot = 5(\mathbf{e} \cdot \mathbf{n}_\odot)\mathbf{e} \times \mathbf{n}_\odot. \tag{C6}$$

Let $\mathbf{e}$ and $\mathbf{j}$ define the positive x- and y-axes of a Cartesian coordinate system and in this system let $\mathbf{n}_\odot = (\cos\psi, \sin\psi)$. Then equation (C6) becomes $(1 + 4e^2)\sin\psi\cos\psi = 0$. Hence either $\sin\psi = 0$ or $\cos\psi = 0$. If $\sin\psi = 0$, $\mathbf{e}$ is parallel or antiparallel to $\mathbf{n}_\odot$, and we return to case (bab), which has no solution. If $\cos\psi = 0$, then $\mathbf{j}$ is parallel or antiparallel to $\mathbf{n}_\odot$, so

$\mathbf{n}_\odot \cdot \mathbf{n}_p = 0$, a special case (planetary obliquity of 90°) that we have already excluded from consideration.

Thus the only eccentric Laplace equilibria are case (aa), in which both $\mathbf{j}$ and $\mathbf{e}$ lie in the principal plane formed by $\mathbf{n}_p$ and $\mathbf{n}_\odot$ (coplanar-coplanar equilibrium); case (ab), in which $\mathbf{j}$ lies in the principal plane and $\mathbf{e}$ is normal to this plane (coplanar-orthogonal equilibrium); or case (baa), in which $\mathbf{e}$ lies in the principal plane and $\mathbf{j}$ is normal to the plane (orthogonal-coplanar equilibrium).

REFERENCES

Borderies, N., & Goldreich, P. 1984, Cel. Mech., 32, 127

Boué, G., & Laskar, J. 2006, Icarus, 185, 312

Breiter, S., & Ratajczak, R. 2005, MNRAS, 364, 1222

Dobrovolskis, A. R., Borderies, N. L., & Steiman-Cameron, T. Y. 1989, Icarus, 81, 132

Ford, E. B., Kozinsky, B., & Rasio, F. A. 2000, ApJ, 535, 385

Goldreich, P. 1965, AJ, 70, 5

Holman, M., Touma, J., & Tremaine, S. 1997, Nature, 386, 254

Kozai, Y. 1962, AJ, 67, 591

Landau, L. D., & Lifshitz, E. M. 1976, Mechanics, 3rd ed. (Amsterdam: Elsevier)

Laplace, P. S. 1805, Mécaniqe céleste, Volume 4, Book 8, (Paris: Courcier)

Milankovich, M. 1939, Bull. Serb. Acad. Math. Nat. A, number 6

Murray, C. D., & Dermott, S. F. 1999, Solar System Dynamics (Cambridge: Cambridge University Press)

Takeda, G., Kita, R., & Rasio, F. A. 2008, ApJ, to be published (arXiv:0802.4088)

Touma, J., & Wisdom, J. 1998, AJ, 115, 1653

Tremaine, S. 1991, Icarus, 89, 85

Ward, W. R. 1981, Icarus, 46, 97

Table 1. Properties of the outer planets

planet	$a_\odot$ (AU)	R_p (km)	J_2	J_2'	obliquity	r_L/R_p	r_H/R_p
Jupiter	5.2029	71492	0.014696	0.045020	3.1°	35.36	743.3
Saturn	9.5367	60330	0.016291	0.070561	26.7°	48.40	1080.1
Uranus	19.189	26200	0.003343	0.018699	97.9°	63.96	2675.1
Neptune	30.070	25225	0.00341	0.024069	29.6°	93.20	4600.8
Pluto	39.482	1151	–	14.296	112.5°	419.6	6935.8

Note. — The planet's semimajor axis and radius are $a_\odot$ and R_p. Obliquity is the angle between the planet's spin and orbital axes, which in the notation of this paper is given by $\phi_\odot = \cos^{-1} \mathbf{n}_p \cdot \mathbf{n}_\odot$. The Laplace radius r_L and Hill radius r_H are defined by equations (24) and (6).